
Performance Evaluation of Data Collection for Out-door Plant Experiments Based on NB-IoT and LTE-M

Masterarbeit zur Erlangung des akademischen Grades

Master of Science

im Studiengang Communication Systems and Networks

an der Fakultät für Informations-, Medien- und Elektrotechnik
der Technischen Hochschule Köln

vorgelegt von: Kai Lübeck
Matrikel-Nr.: 11127675
Adresse: Zülpicher Straße 231
50937 Köln
kai.luebeck@smail.th-koeln.de

eingereicht bei: Prof. Dr. Uwe Dettmar
Zweitgutachter*in: Prof. Dr. Harald Elders-Boll

Köln, 14.08.2025

Contents

1	Introduction	1
1.1	Motivation	1
1.2	Related Work	2
1.2.1	Protocol Performance in Cellular IoT Networks	2
1.2.2	Energy Consumption Analysis	2
1.2.3	Coverage and Capacity Analysis	3
1.2.4	Similarities and Differences	3
1.2.5	Research Gap and Contribution	3
1.3	Objectives	3
1.4	Structure of the Thesis	5
2	Theoretical Background	6
2.1	NB-IoT	6
2.1.1	Frequency Usage and Deployment Modes	6
2.1.2	Physical Layer and Modulation Schemes	6
2.1.3	Channel Coding and Error Correction	7
2.1.4	Bandwidth, Throughput, and Latency	7
2.1.5	Security Aspects	8
2.1.6	Power Consumption and Energy Efficiency	8
2.1.7	Network Parameter Evaluation	9
2.1.8	Summary	9
2.2	LTE-M	9
2.2.1	Frequency Usage and Deployment Modes	9
2.2.2	Physical Layer and Modulation Schemes	10
2.2.3	Channel Coding and Error Correction	10
2.2.4	Bandwidth, Throughput, and Latency	11
2.2.5	Mobility and Handover Support	11
2.2.6	Security Aspects	11
2.2.7	Power Consumption and Energy Efficiency	12
2.2.8	Network Parameter Evaluation	12

2.2.9	Summary	12
2.3	MQTT	12
2.3.1	Architectural Model	13
2.3.2	Transport Layer and Connection Establishment	13
2.3.3	Messaging and Quality of Service	13
2.3.4	Performance Considerations in Connection Stability	14
2.3.5	Visualization of Connection Establishment	14
2.3.6	Security Features and Mechanisms	14
2.3.7	Summary	14
2.4	LWM2M	14
2.4.1	Architectural Model	17
2.4.2	Transport Layer and Connection Establishment	17
2.4.3	Messaging and QOS	17
2.4.4	Performance Considerations in Connection Stability	18
2.4.5	Visualization of Connection Phases	18
2.4.6	Security Features and Mechanisms	18
2.4.7	Summary	18
2.5	Comparison of NB-IoT and LTE-M	18
2.6	Comparison of MQTT and LwM2M	20
3	Implementation	22
3.1	Hardware Overview	22
3.2	Software Overview	22
3.2.1	Operating System and SDK	24
3.2.2	Development Environment	24
3.2.3	GNSS and AGNSS Integration	24
3.2.4	Communication Infrastructure	24
3.2.5	Data Storage and Backend Processing	25
3.2.6	Multi-Board Setup	25
3.3	Measurement setup	25
3.3.1	Firmware Workflow and Test Procedure	26
3.3.2	Data Collection and Logging Framework	27
3.3.3	Modem Trace Analysis	28
3.3.4	Parallelized Testing	28
3.4	Challenges	28

3.4.1	Modem Trace Extraction and Analysis	29
3.4.2	Throughput Measurement Implementation	29
3.4.3	Measurement Framework Stability and Automation	30
4	Measurements	31
4.1	Data Processing and Analysis Methodology	35
4.2	Measurement Results	39
4.2.1	Communication Technology comparisons	39
4.2.2	Protocol and Technology Combination Analysis	54
5	Discussion	67
5.1	Interpretation of results	67
5.1.1	Signal Quality and Coverage Performance	67
5.1.2	Power Consumption and Energy Efficiency	68
5.1.3	Connection Establishment and Throughput Performance	68
5.1.4	Limitations of the Study	69
6	Conclusion	71
6.1	Summary of Findings	71
6.1.1	Communication Technology Performance	71
6.1.2	Protocol Performance Across Technologies	72
6.1.3	Technology and Protocol Recommendations	72
6.1.4	Research Contributions	73
7	Outlook	75
Tools Used		76
8	Acknowledgements	77

1. Introduction

1.1 Motivation

This project was motivated by the increasing need to collect reliable, high-resolution environmental data for plant experiments performed under outdoor conditions. Accurate monitoring of climate parameters is essential to understanding how plants respond to environmental changes, especially in the context of climate change and ecological research. This thesis is based on a collaboration between the Digital Communication Department at TH Köln and the Biology Department at Universität zu Köln. The collaboration focuses on improving methods for recreating real-world climate conditions in controlled environments.

The project's primary objective is to provide a framework for the collection of a wide range of climate parameters in outdoor settings. The goal of this project is to replicate these outdoor conditions within controlled indoor environments, such as climate chambers. This study will provide a scientific basis for analyzing the influence of climate change and various biological approaches on plant growth under realistic conditions.

In previous research, sensor systems for plant experiments were operated in closed indoor environments where robust internet infrastructure, such as Wireless Fidelity (WiFi) or Ethernet, was available. However, as research continues to expand into outdoor applications, the lack of internet connectivity becomes a significant challenge for data acquisition and transmission. The development of technologies such as Narrowband Internet of Things (NB-IoT) and Long Term Evolution (LTE) has led to the promising solution of reliable and energy-efficient communication in remote and distributed sensor networks.

While prior studies have established a solid base of knowledge regarding the performance characteristics of Low Power Wide Area Network (LPWAN) technology, a review of the existing literature reveals significant gaps in the evaluation of these technologies in outdoor settings. Prior studies have addressed specific aspects, including protocol efficiency, energy consumption analysis, and rural coverage planning. However, these studies lack a systemic analysis that integrates the performance of communication technology and the behavior of protocols under real-world outdoor conditions. Additionally, the concurrent evaluation of radio frequency parameters, protocol-specific metrics, and practical performance characteristics across multiple geographic locations has not been extensively explored in the existing research.

By testing NB-IoT and LTE technologies in combination with Message Queuing Telemetry Transport (MQTT) and Lightweight Machine to Machine (LWM2M) protocols, this project aims to enable continuous collection of diverse sensor data, supporting more advanced analyses of plant-environment interactions. The research evaluates the performance characteristics of

these protocol-technology combinations to determine optimal configurations for outdoor deployments. This work is expected to contribute to the scientific understanding of how climate variables influence plant growth while providing practical guidance for deploying reliable sensor networks in challenging outdoor environments using Internet of Things (IoT) communication protocols.

1.2 Related Work

This section reviews related studies investigating LPWAN technology and IoT protocol performance characteristics, providing context for the findings presented in this thesis.

1.2.1 Protocol Performance in Cellular IoT Networks

A study by Parmigiani and Dettmar evaluated LWM2M and MQTT performance over NB-IoT and LTE networks, focusing on energy consumption and traffic efficiency [9]. The authors performed measurements using Raspberry Pi hardware with Quectel BG96 modems across European cellular networks in Slovakia and Italy. The study focuses on three scenarios: initial connection setup, single client-to-server messages, and steady-state updates under different security levels (no-security, Pre-Shared Key (PSK), certificates).

Key Findings: LWM2M demonstrated superior efficiency during initial connection establishment, transferring 82% and 61% fewer bytes than MQTT over LTE and NB-IoT respectively. MQTT outperformed LWM2M for large payload transmissions, consuming 20% less energy for single message transfers. For small payloads below MTU threshold, LWM2M showed 44% lower energy consumption. During steady-state operations, the effect of the chosen protocol became irrelevant due to the effects of the Radio Resource Control (RRC) inactivity timer.

1.2.2 Energy Consumption Analysis

A energy consumption study by Vomhoff et al. investigated power characteristics of NB-IoT and Long Term Evolution for Machines (LTE-M) using Arduino MKR NB 1500 platforms with high-precision Tinkerforge measurement equipment [13]. The research created a cost-efficient testbed achieving 1mW energy monitoring resolution and evaluated network attachment procedures and data transmission with Hypertext Transfer Protocol (HTTP) and MQTT protocols.

Key Findings: Network attachment consumed significantly more energy for NB-IoT compared to LTE-M, while NB-IoT demonstrated superior idle efficiency. Devices maintaining long-term connections benefited from NB-IoT, whereas applications requiring frequent reconnections achieved lower consumption with LTE-M. MQTT had higher connection overhead than HTTP but provided more efficient data transmission for smaller payloads.

1.2.3 Coverage and Capacity Analysis

A rural deployment study by Lauridsen et al. investigated LTE and NB-IoT performance across 800 km² of Danish territory using commercially deployed base station configurations and calibrated propagation models [2]. The simulation-based approach incorporated 71 sectors with realistic antenna patterns, transmit power configurations, and digital elevation maps, calibrated against drive test measurements.

Key Findings: LTE achieved 99.9% outdoor coverage while NB-IoT provided superior deep indoor performance with 164 dB Maximum Coupling Loss versus LTE's 156 dB MCL. Under challenging indoor conditions, LTE supported 80,000 devices per sector versus 5,000 for NB-IoT with full security protocols. NB-IoT devices consumed 2-6 times more power than LTE primarily due to RRC delay overheads, though battery life estimates exceeded 5 years.

1.2.4 Similarities and Differences

All three studies share the same objective of empirically evaluating NB-IoT and LTE performance characteristics, using real-world measurement approaches rather than theoretical analysis. The studies consistently identify energy efficiency trade-offs between the technologies, with NB-IoT demonstrating coverage advantages at the cost of higher connection overhead.

Key differences include hardware platforms (Raspberry Pi, Arduino, simulation), geographic focus (European multi-location, single testbed, rural Denmark), and evaluation scope (protocol comparison, energy analysis, coverage planning). The measurement approaches vary from direct hardware measurements to calibrated simulations, providing diverse perspectives on technology performance.

1.2.5 Research Gap and Contribution

The reviewed literature establishes foundational understanding of LPWAN performance trade-offs but reveals gaps in outdoor deployment evaluation. While existing studies focus on specific aspects (protocol efficiency, energy consumption, rural coverage), none provide integrated analysis of radio frequency parameters, protocol behavior, and practical performance metrics under real-world outdoor conditions. The current thesis addresses this gap by performing systematic outdoor measurements that simultaneously analyze cellular technology performance and protocol interaction dependencies, providing practical guidance for outdoor environmental monitoring deployments.

1.3 Objectives

The present thesis is an evaluation of the performance of two cellular technologies, NB-IoT and LTE, in the context of outdoor plant monitoring. The study focuses on the suitability of these

technologies when used with two popular IoT communication protocols: MQTT and LWM2M. The objective of this study is to determine efficient, reliable, and context-appropriate combinations of protocol and technology for transmitting data in constrained outdoor environments. This study addresses critical gaps identified in the existing literature regarding the comparative performance of MQTT and LWM2M under real-world conditions, especially over narrowband cellular communication links. Although prior studies have shown that LWM2M offers enhanced efficiency during the establishment of connections and that MQTT performs more effectively for transmitting large payloads, these studies have been restricted to specific deployment scenarios or have concentrated on individual performance aspects, such as energy consumption or the analysis of rural coverage. The performance boundaries under which MQTT could outperform CoAP-based LWM2M despite its theoretical inefficiencies, namely, overhead and connection-oriented nature, have not been systematically evaluated across outdoor deployment conditions. Such conditions include radio frequency parameters, protocol behavior, and practical performance metrics.

Furthermore, the efficacy of protocol implementation is dependent on the characteristics of the underlying cellular technology. However, no study has yet provided an integrated analysis of all four protocol-technology combinations under identical environmental conditions. Those combinations are NB-IoT/MQTT, NB-IoT/LWM2M, LTE/MQTT and LTE/LWM2M. A review of the existing literature reveals a consistent identification of trade-offs between technologies in terms of energy efficiency. However, an evaluation of the dependencies between protocols and technologies is lacking. Such an evaluation is critical for informed deployment decisions in outdoor monitoring scenarios.

A key component of the project was the development of a robust, automated measurement setup which includes hardware as well as software, that addresses several limitations observed in previous studies. Those limitations are the fact that most of the existing research if focusing on a single metric or performance indicator, while this study aims to include a huge variety of metrics. The system's design was based on the principle of reproducibility, which aimed to ensure consistent testing across different hardware configurations, communication protocols, and network environments. A primary emphasis was placed on the aggregation and structuring of collected data to support cross-parameter analysis. The resulting dataset includes a wide range of parameters, ranging from signal quality and connection metrics for example snr, rsrp, rsrq to protocol-specific metrics such as timing or latency. The collected data should also be a resource for future research, enabling further interpretation and analysis that goes beyond the scope of this thesis. Upon completion of the project, the dataset will be open-sourced to support open scientific research.¹

To achieve the research objective and address the identified research gaps, the following measurable outcomes are targeted:

¹<https://github.com/MrPink1996/Performance-Evaluation-of-Data-Collection-for-Outdoor-Plant-Experiments-Based-on-NB-IoT-and-LTE-M>

- Perform a quantitative evaluation of key network performance indicators, including data throughput, end-to-end latency, connection setup time, stability, and coverage, under changing environmental and locational conditions across multiple geographic measurement points.
- Perform simultaneous comparison of MQTT and LWM2M protocol behavior on both NB-IoT and LTE-M networks to establish protocol-technology interaction dependencies.
- Identify deployment-specific trade-offs, such as protocol overhead, energy efficiency, and communication reliability, in outdoor experimental setups through integrated analysis of radio frequency parameters and protocol-specific metrics.
- Determine optimal protocol-technology combinations for specific use cases within agricultural and environmental IoT applications through empirical research that addresses gaps in existing literature.

1.4 Structure of the Thesis

The following chapters are organized to provide a detailed overview of the thesis.

Chapter 2 introduces the theoretical background on NB-IoT, LTE-M, MQTT, and LWM2M. Chapter 3 describes the implementation, including hardware and software components, the measurement setup, and the challenges faced during the project.

Chapter 4 presents the measurement results and describes the data analysis methods.

Chapter 5 discusses the interpretation of results, compares NB-IoT and LTE-M as well as MQTT and LWM2M, and addresses the limitations of the study.

Chapter 6 summarizes the findings and offers recommendations for future work.

Finally, Chapter 7 provides an outlook on potential future developments in data collection for outdoor plant experiments.

2. Theoretical Background

2.1 NB-IoT

NB-IoT, classified as LTE Category NB1 (Cat-NB1), is a cellular communication technology standardized by the 3rd Generation Partnership Project (3GPP) as part of the Release 13 specifications [3]. It is specifically designed to support massive Machine-Type Communication (Massive Machine-Type Communication (mMTC)) applications within the IoT ecosystem. NB-IoT addresses critical requirements such as extended coverage, low power consumption, massive device connectivity, and optimized network resource utilization, making it suitable for scenarios such as smart metering, environmental monitoring, and asset tracking.

2.1.1 Frequency Usage and Deployment Modes

NB-IoT operates in licensed spectrum within existing cellular frequency bands and can be deployed in three distinct modes [3]:

- **In-band deployment:** Utilizes resource blocks within an existing LTE carrier's bandwidth, allowing NB-IoT to coexist with LTE users.
- **Guard-band deployment:** Fills up unused resource blocks in the guard bands of LTE carriers to avoid interference and improve spectral efficiency.
- **Standalone deployment:** Operates independently within reused Global System for Mobile Communications (GSM) spectrum (e.g., a 200 kHz GSM channel), making use of legacy infrastructure and providing deployment flexibility in rural or remote areas.

NB-IoT uses a narrow carrier bandwidth of 180 kHz, equivalent to a single LTE Physical Resource Block (PRB). This design choice ensures cost-efficiency in transceiver hardware and improves indoor penetration by concentrating energy over a narrowband.

2.1.2 Physical Layer and Modulation Schemes

The physical layer of NB-IoT is based on LTE technology, with simplifications for cost and coverage optimization [8]. It supports different modulation and access schemes for uplink and downlink:

- **Downlink:** NB-IoT employs Orthogonal Frequency Division Multiple Access (OFDMA) with a subcarrier spacing of 15 kHz, matching LTE. OFDMA divides the spectrum into orthogonal subcarriers, allowing multiple users to transmit simultaneously without mutual interference. The modulation scheme used in the downlink is typically Quadrature Phase Shift Keying (QPSK), ensuring a balance between spectral efficiency and robustness.
- **Uplink:** Two modes are supported: single-tone and multi-tone transmissions. Uplink access uses Single Carrier Frequency Division Multiple Access (SC-FDMA), which, unlike OFDMA, transmits data in a single carrier with a lower Peak-to-Average Power Ratio (PAPR), ideal for energy-constrained IoT devices. Depending on configuration:
 - **Single-tone:** Uses one subcarrier (3.75 kHz or 15 kHz) with Binary Phase Shift Keying (BPSK) or QPSK modulation.
 - **Multi-tone:** Uses up to 12 subcarriers, each spaced at 15 kHz, occupying the full 180 kHz bandwidth, with QPSK modulation.

These physical layer characteristics are designed to enhance coverage and minimize energy consumption, even in conditions with poor signal strength [8].

2.1.3 Channel Coding and Error Correction

NB-IoT uses robust error correction and coding techniques derived from LTE, which have been adapted for low data rates and enhanced coverage [8].

- **Downlink:** Employs Turbo codes, which are powerful Forward Error Correction (FEC) schemes known for near-Shannon-limit performance.
- **Uplink:** Uses convolutional codes, which are less complex than Turbo codes, making them suitable for energy-efficient uplink transmissions.

Furthermore, repetition coding is a fundamental technique in the field of NB-IoT, where messages are transmitted multiple times to improve reliability in low Signal-to-Noise Ratio (SNR) environments. This repetition has been shown to improve coverage by up to 20 dB in comparison with standard LTE [3].

2.1.4 Bandwidth, Throughput, and Latency

Due to its narrow bandwidth of 180 kHz, NB-IoT offers modest data throughput but is sufficient for most IoT use cases [3]:

- **Downlink:** Peak data rate up to 127 kbps.
- **Uplink:** Peak rate up to 159 kbps using 12-tone multi-tone transmission. In single-tone mode, uplink rates are significantly lower, typically around 66 kbps.

Latency in NB-IoT is optimized for small, infrequent data transmissions. Depending on network conditions, repetition, and power-saving configurations, latency ranges from 1.6 s to over 10 s.

2.1.5 Security Aspects

The security architecture of NB-IoT is derived from LTE, thereby ensuring robust protection for user and signaling data [21].

- **Mutual authentication:** Between the device and the network using standardized 3GPP Authentication and Key Agreement (AKA) protocols.
- **Encryption:** Based on secure algorithms like SNOW 3G (SNOW) and Advanced Encryption Standard (AES), protecting data confidentiality.
- **Integrity protection:** Ensures signaling messages are not altered in transmissions.
- **Dynamic key management:** Cryptographic keys are generated and refreshed periodically during secure sessions.

The mechanisms, when considered together, ensure secure end-to-end communication suitable for critical IoT applications.

2.1.6 Power Consumption and Energy Efficiency

The design of NB-IoT is focused on energy-constrained IOT devices [6]. The primary mechanisms that contribute to extending battery life beyond 10 years are as follows:

- **Power Saving Mode (PSM):** The device enters a deep sleep state while remaining registered to the network. No downlink reception occurs, reducing power draw to microampere levels.
- **Extended Discontinuous Reception (eDRX):** The device periodically wakes up to check for messages. Idle cycles are extended up to several minutes, dramatically lowering average power consumption.

These features are critical for devices deployed in remote areas where frequent maintenance is impractical [6].

2.1.7 Network Parameter Evaluation

NB-IoT performance can be analyzed using standard communication metrics [3]:

- **Spectral Efficiency:** Although NB-IoT uses narrow bandwidth, its modulation and coding schemes ensure spectral efficiency around 0.2-1.4 bit/s/Hz depending on link conditions.
- **Coverage Enhancement:** Link budget improvements of up to 20 dB allow connectivity in basements, rural, and underground locations.
- **Massive Connectivity:** More than 50,000 devices per cell should be supported.
- **Reliability:** Enhanced by Hybrid Automatic Repeat reQuest (HARQ), convolutional coding, and repetition techniques.
- **Latency-Throughput Tradeoff:** Although not suitable for real-time applications, it demonstrates optimal performance in energy-efficient, delay-tolerant communication.

2.1.8 Summary

It is widely acknowledged that NB-IoT plays a fundamental role in ensuring the effective operation of large-scale IoT networks [3]. The device's narrowband operation, simplified physical layer, and optimized power consumption contribute to secure, long-range, and low-cost connectivity. Despite its constrained throughput and real-time capabilities, the device demonstrates notable strengths in scenarios that require extended battery life, extensive coverage, and secure low-bandwidth data exchange.

2.2 LTE-M

LTE-M, specifically LTE Category M1 (Cat-M1), is a LPWAN technology that has been standardized by the 3GPP in Release 13 [5]. It is designed to support IoT applications requiring higher data rates, reduced latency, and mobility support compared to NB-IoT. Positioned between legacy LTE and NB-IoT, LTE-M offers a balanced trade-off between throughput and power efficiency for use cases such as wearables, asset tracking, and Voice over LTE (VoLTE)-enabled sensors.

2.2.1 Frequency Usage and Deployment Modes

LTE-M operates within licensed LTE spectrum and supports [5]:

- **In-band deployment:** LTE is integrated into the same LTE carrier bandwidth as traditional LTE traffic, taking advantage of dynamic resource allocation across the shared spectrum.

Unlike NB-IoT, LTE-M does not support guard-band or standalone deployment modes. It uses a bandwidth of 1.4 MHz, equivalent to six LTE PRB, enabling higher data rates and improved spectral efficiency.

2.2.2 Physical Layer and Modulation Schemes

The physical layer of LTE-M is largely derived from LTE, with specific optimizations for the purpose of reducing device complexity and enhancing power efficiency [5].

- **Downlink:** Uses Orthogonal Frequency Division Multiplexing (Orthogonal Frequency Division Multiplexing (OFDM)) with a subcarrier spacing of 15 kHz, identical to LTE. Supported modulation schemes include QPSK and 16-Quadrature Amplitude Modulation (QAM), enabling a good balance between spectral efficiency and robustness.
- **Uplink:** Uses SC-FDMA with 15 kHz subcarrier spacing. It supports both QPSK and 16-QAM, allowing scalable uplink data rates based on channel conditions and power requirements.

In contrast to the NB-IoT, the LTE-M offers support for mobility and higher-order modulation, making it well-suited for devices that require real-time data exchange and roaming capabilities.

2.2.3 Channel Coding and Error Correction

LTE-M reuses LTE's robust error correction schemes [5]:

- **Downlink:** Turbo coding provides powerful FEC, ensuring data integrity in poor channel conditions.
- **Uplink:** Control channels often use convolutional codes for lower computational complexity, while data channels continue to use Turbo codes.

HARQ is also implemented, combining FEC with retransmission for improved reliability.

2.2.4 Bandwidth, Throughput, and Latency

With its 1.4 MHz bandwidth, LTE-M offers significantly higher throughput and lower latency than NB-IoT [5]:

- **Downlink:** Peak throughput of up to 1 Mbps, sufficient for voice, messaging, and Firmware Over-The-Air (FOTA) updates.
- **Uplink:** Data rates up to 375 kbps, depending on modulation and resource allocation.
- **Latency:** Typically between 10 ms and 15 ms, which supports delay-sensitive applications such as alarms or voice.

The selected performance metrics are well-suited for use cases which require moderate, bidirectional data flows.

2.2.5 Mobility and Handover Support

LTE-M has been developed to support continuous cell reselection and handover, including idle and connected mode mobility, making it suitable for mobile IoT applications such as vehicle tracking, logistics, and mobile health monitoring [5]. Additionally, it supports VoLTE, allowing for real-time voice communication over cellular IoT devices.

2.2.6 Security Aspects

LTE-M maintains LTE's full security architecture [19]:

- **Mutual authentication:** Ensures secure identity verification via the standardized 3GPP AKA protocol.
- **Encryption and integrity:** Both user and signaling data are protected with AES and SNOW algorithms.
- **Key management:** Session keys are dynamically generated and periodically refreshed to ensure confidentiality.

This robust security framework supports trusted communication in critical and sensitive IoT applications.

2.2.7 Power Consumption and Energy Efficiency

While offering higher link throughput, the system still focuses on energy-efficient operation through the following mechanisms [14]:

- **PSM:** Allows the device to enter a deep-sleep state while retaining network context, minimizing energy consumption between transmissions.
- **eDRX:** Reduces power usage by decreasing the frequency of downlink listening periods, adjustable based on application needs.

These features support battery lifetimes of up to 10 years, depending on the data transmission profile [14].

2.2.8 Network Parameter Evaluation

Key performance indicators for LTE-M include [5]:

- **Spectral Efficiency:** Higher than NB-IoT due to wider bandwidth and support for 16-QAM, typically around 1-3 bit/s/Hz depending on link conditions.
- **Coverage Enhancement:** Provides up to 15 dB gain over legacy LTE, enabling reliable connections in deep indoor and remote environments.
- **Latency-Throughput Tradeoff:** Offers improved latency and throughput, but with slightly higher energy cost compared to NB-IoT.

2.2.9 Summary

The LTE-M standard is a technological advancement that increases LTE's capabilities to the Internet of Things (IoT) domain, thereby enabling applications that require mobility, moderate data rates, and low latency [5]. The device's compatibility with existing infrastructure originates from its support for in-band and guard-band deployment in combination with standard LTE modulation and coding schemes. While not as energy-optimized as NB-IoT, its wider range of features makes it an ideal solution for a wide range of smart connected devices.

2.3 MQTT

The MQTT protocol is a lightweight, publish-subscribe network protocol designed for efficient message transport between devices in distributed systems [20]. It is optimized for resource-constrained environments and communication over low-bandwidth, high-latency, or unreliable networks, making it suitable, especially for IoT applications and Machine to Machine (M2M) communication [4].

2.3.1 Architectural Model

MQTT is based on a broker-client architecture, which differs fundamentally from traditional client-server models [4]. Its core components include:

- **Broker:** A central entity that receives all messages, filters them according to their topics, and forwards them to subscribed clients.
- **Clients:** Devices or applications that publish data to topics or subscribe to topics to receive data.

Communication occurs over *topics*, which are hierarchical UTF-8 strings. Clients publish messages to a topic, and subscribers receive those messages asynchronously. This decoupling made scalable and flexible communication patterns possible.

2.3.2 Transport Layer and Connection Establishment

MQTT uses Transmission Control Protocol (TCP) as its transport layer protocol [4]. Key aspects include:

- **Three-way handshake:** Required to establish a TCP connection before MQTT communication.
- **Connection state maintenance:** TCP maintains permanent connections, allowing continuous sessions essential for IoT use cases.

Frequent connection disruptions (e.g., in wireless networks) require repeated handshakes, increasing latency and resource consumption.

2.3.3 Messaging and Quality of Service

MQTT communication involves several control packets:

- **CONNECT, PUBLISH, SUBSCRIBE, DISCONNECT**

It supports three QoS levels [20]:

1. **QoS 0 (At most once):** Unreliable but low overhead.
2. **QoS 1 (At least once):** Reliable with possible duplication.
3. **QoS 2 (Exactly once):** Most reliable, highest overhead.

These allow flexibility between reliability, latency, and resource use.

2.3.4 Performance Considerations in Connection Stability

Unstable connections lead to increased overhead from repeated handshakes and session reinitialization, reducing throughput and increasing energy use. Optimizing connection persistence is critical in such scenarios [4].

2.3.5 Visualization of Connection Establishment

Figures 2.1 and 2.2 illustrating client-broker interaction including TCP handshake, MQTT session setup, and Quality of Service (QoS)-based message flow.

2.3.6 Security Features and Mechanisms

While MQTT is lightweight and lacks built-in security, typical implementations rely on [20]:

- **Transport Layer Security (TLS) encryption**
- **Client authentication (username/password, certificates)**
- **Broker-side access control**
- **Message integrity/replay protection via TLS**

Security depends on proper configuration of these additional mechanisms.

2.3.7 Summary

MQTT enables lightweight, publish-subscribe messaging, which is well-suited for IoT applications [4]. It is not equipped with built-in security features, but it can be secured through the use of TLS and broker-based controls. This approach provides scalable and secure communication within constrained environments.

2.4 LWM2M

The LWM2M protocol is a standardized protocol developed by the Open Mobile Alliance for the efficient management of resource-constrained IoT devices [7]. This system supports remote configuration, telemetry, and lifecycle management [22].

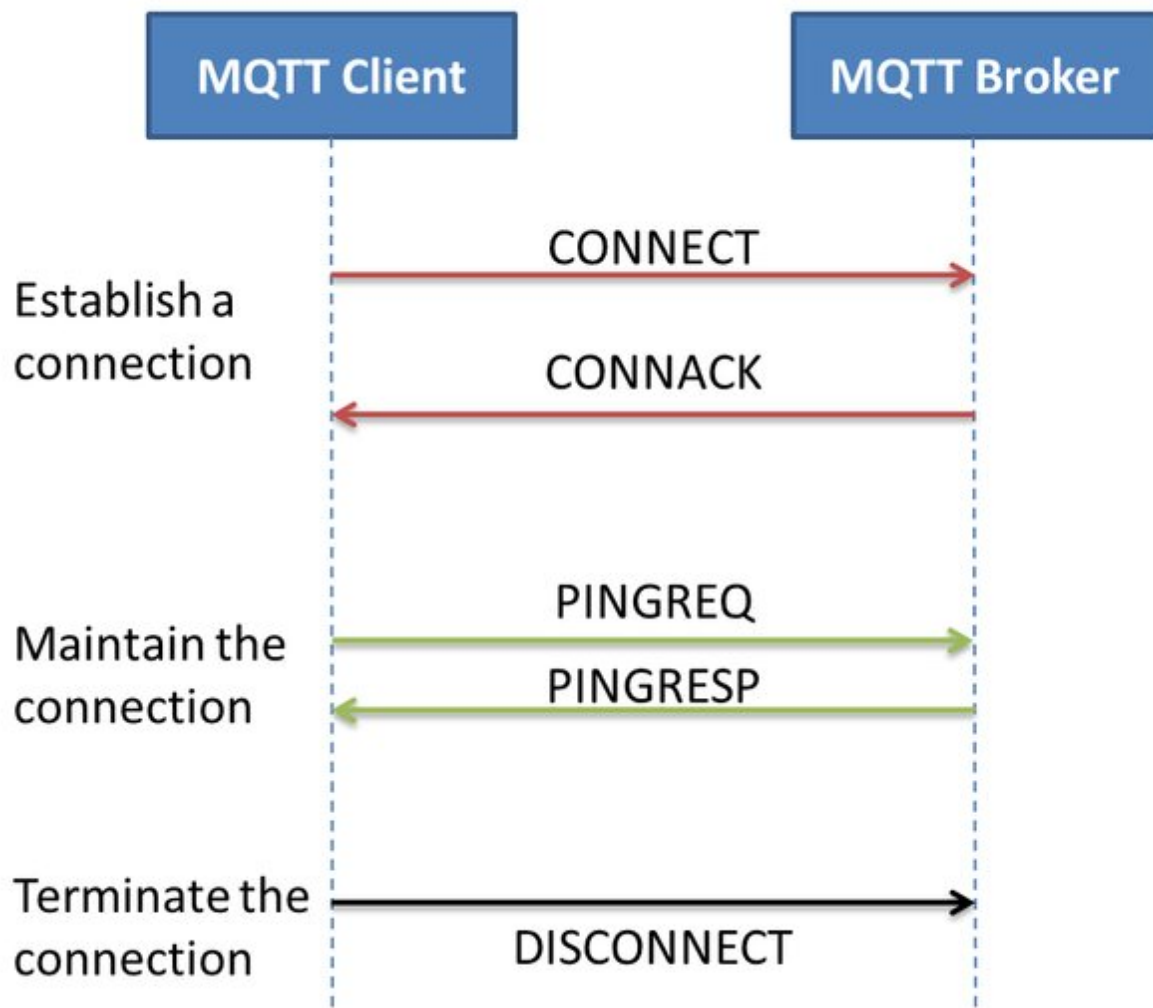


Figure 2.1: **MQTT Connection Establishment**

The picture shows the typical phases of the client-broker connection in MQTT. [1]

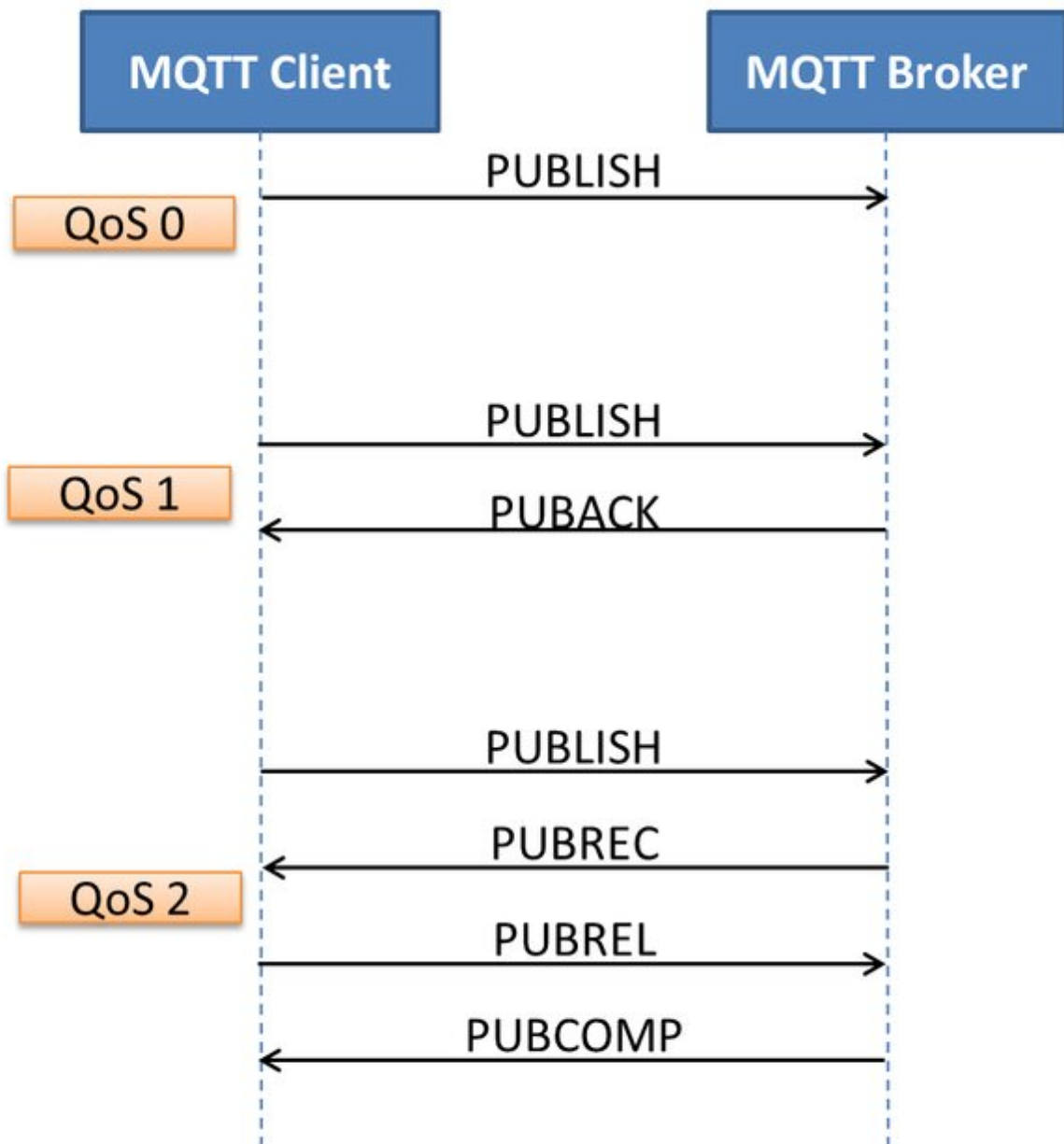


Figure 2.2: **MQTT Messaging**

The picture shows the behavior when transmitting messages with different QoS parameters.
[1]

2.4.1 Architectural Model

LwM2M follows a *client-server architecture*, focusing on remote device management [7]. Core elements include:

- **LwM2M Client:** Usually an embedded device or sensor that exposes resources.
- **LwM2M Server:** Manages clients by reading/writing values and issuing commands.

The model is based on hierarchical *objects*, *instances*, and *resources*, enabling standardized device interaction.

2.4.2 Transport Layer and Connection Establishment

LWM2M uses the Constrained Application Protocol (CoAP) over User Datagram Protocol (UDP) [7]:

- **UDP transport:** Reduces overhead and supports faster communication compared to TCP.
- **Reliability mechanisms:** CoAP provides confirmable messages, retransmissions, and deduplication to ensure reliable communication.

This enables efficient, low-latency communication suitable for battery-powered devices.

2.4.3 Messaging and QOS

LWM2M messaging uses CoAP's RESTful methods (GET, POST, PUT, DELETE) and includes [7]:

- **Read/write operations**
- **Execute commands**
- **Bootstrap procedures**
- **Observation of resources**

Quality and reliability are handled via CoAP's confirmable/non-confirmable messages. While not using QoS levels like MQTT, it achieves similar guarantees through message acknowledgments and retransmissions.

2.4.4 Performance Considerations in Connection Stability

Operating over UDP allows for low overhead but requires robust retransmission logic. The lightweight reliability mechanisms of CoAP serve to reduce the impact of interrupted connectivity, thereby enabling LWM2M to operate over unreliable links while preserving energy efficiency [7].

2.4.5 Visualization of Connection Phases

Analogous to MQTT, LWM2M involves a multi-step process:

- UDP transmission initiation
- Datagram Transport Layer Security (DTLS) handshake (if security enabled)
- CoAP-based messaging and observation
- Optional bootstrap and resource management

2.4.6 Security Features and Mechanisms

LWM2M provides strong built-in security [7]:

- **DTLS encryption** over UDP
- **Authentication:** Pre-shared keys, raw public keys, or certificates
- **Fine-grained access control** on resources
- **Replay protection** via DTLS features

These security features are fundamental to the protocol and are essential for protecting managed devices from unauthorized access or control.

2.4.7 Summary

LWM2M is a comprehensive protocol for managing constrained IoT devices [22]. The CoAP messaging over UDP, hierarchical resource modeling, and robust security via DTLS enable scalable and secure device management in distributed IoT environments [7].

2.5 Comparison of NB-IoT and LTE-M

Table 2.1: Comparison of Key Features between LTE-M and NB-IoT

Feature	LTE-M	NB-IoT
3GPP Category	Cat-M1	Cat-NB1
Carrier Bandwidth	1.4 MHz (6 PRBs)	180 kHz (1 PRB)
Deployment Modes	In-band only	In-band, Guard-band, Standalone (re-farmed GSM)
Modulation Schemes	QPSK, 16-QAM (DL/UL)	BPSK, QPSK (mostly)
Peak Downlink Throughput	Up to 1 Mbps	Up to 127 kbps
Peak Uplink Throughput	Up to 375 kbps	Up to 159 kbps (12-tone), 66 kbps (single-tone)
Latency	Typically 10–15 ms	Typically 1.6 s to 10 s
Mobility Support	Full LTE mobility and handover support	Limited mobility, no handovers
Coverage Enhancement	Approx. 15 dB over LTE	Up to 20 dB over LTE
Power Saving Features	PSM, eDRX	PSM, eDRX
Security	LTE-grade (AKA, encryption, integrity)	LTE-grade (AKA, encryption, integrity)
Typical Applications	Asset tracking, wearables, VoLTE	Smart metering, environmental monitoring
Device Complexity	Moderate	Very low

2.6 Comparison of MQTT and LwM2M

Table 2.2: Comparison of Key Features between LwM2M and MQTT

Feature	LwM2M	MQTT
Protocol Type	Device management and telemetry	Lightweight messaging protocol (telemetry)
Transport Layer	UDP (via CoAP)	TCP
Communication Model	Client-Server (RESTful)	Broker-based Publish/-Subscribe
Data Model	Hierarchical: Object / Instance / Resource	Flat, topic-based string hierarchy
Message Encoding	Compact binary (Efficient XML Interchange or CBOR)	Text or binary payloads, no strict structure
Reliability Mechanism	CoAP confirmable messages, retransmission, deduplication	QoS levels 0 (at most once), 1 (at least once), 2 (exactly once)
Security	Built-in DTLS (PSK, RPK, X.509); integrated replay protection	Relies on TLS and broker-side access control
Device Management	Full: provisioning, firmware update, resource monitoring	Not natively supported; possible via custom payloads
Suitability for Constrained Devices	High (optimized for low-power, low-memory devices)	Moderate (requires persistent TCP connection)
Connection Overhead	Low (UDP, stateless, no keep-alive)	Moderate (TCP handshake and keep-alive required)
Session Persistence	Stateless by design; can reconnect without session context	Stateful; relies on persistent TCP session
Use Cases	Device lifecycle management, telemetry, firmware updates	Sensor telemetry, alerts, asynchronous event notifications
Standardization Body	OMA SpecWorks	OASIS

3. Implementation

3.1 Hardware Overview

The implementation and testing of this project was carried out using the nRF9160 Development Kit from Nordic Semiconductor. The core of the kit is the nrf9160 System on a Chip (SoC), which integrates an energy-efficient Arm Cortex-M33 application processor and a dedicated cellular modem supporting both NB-IoT (Cat-NB1) and LTE-M (Cat-M1) technologies. The nRF9160 System in Package (SiP) is specifically designed to support Long-Term Evolution (LTE) Cat-M1 and Cat-NB1, providing full LPWAN connectivity capabilities for IoT applications.

The nRF9160 SoC integrates multiple peripheral interfaces for sensor integration and includes an integrated Global Positioning System (GPS) module, which enables precise geolocation functionality. This feature is advantageous for mobile or spatially distributed IoT deployments. Furthermore, the development board includes a distinct nRF52840 SoC that provides support for Bluetooth Low Energy (BLE) and Near Field Communication (NFC), though these wireless interfaces are not used in this project.

The nRF9160 Development Kit is well-suited for prototyping and evaluating IoT applications in constrained environments due to its low-power operation, wide-area connectivity, and flexible peripheral support. This performance-focused study identified the nRF9160 Development Kit as an optimal selection. As illustrated in Figure 3.1, a general overview of the hardware is provided.

For the purpose of this study, two identical nRF9160 Development Kits were used in parallel: one configured to run an LWM2M-based implementation, and the other dedicated to MQTT communication combined with Global Navigation Satellite System (GNSS)-based location tracking. This enabled the simultaneous evaluation of both protocol stacks under comparable field conditions.

3.2 Software Overview

The software environment used in this project was designed to align with the hardware capabilities of the NRF9160 and to support robust, low-power communication protocols suitable for IoT deployments. This chapter presents an overview of the operating system, development tools, protocol stacks, backend infrastructure, and data analysis frameworks used during the implementation and testing phases.

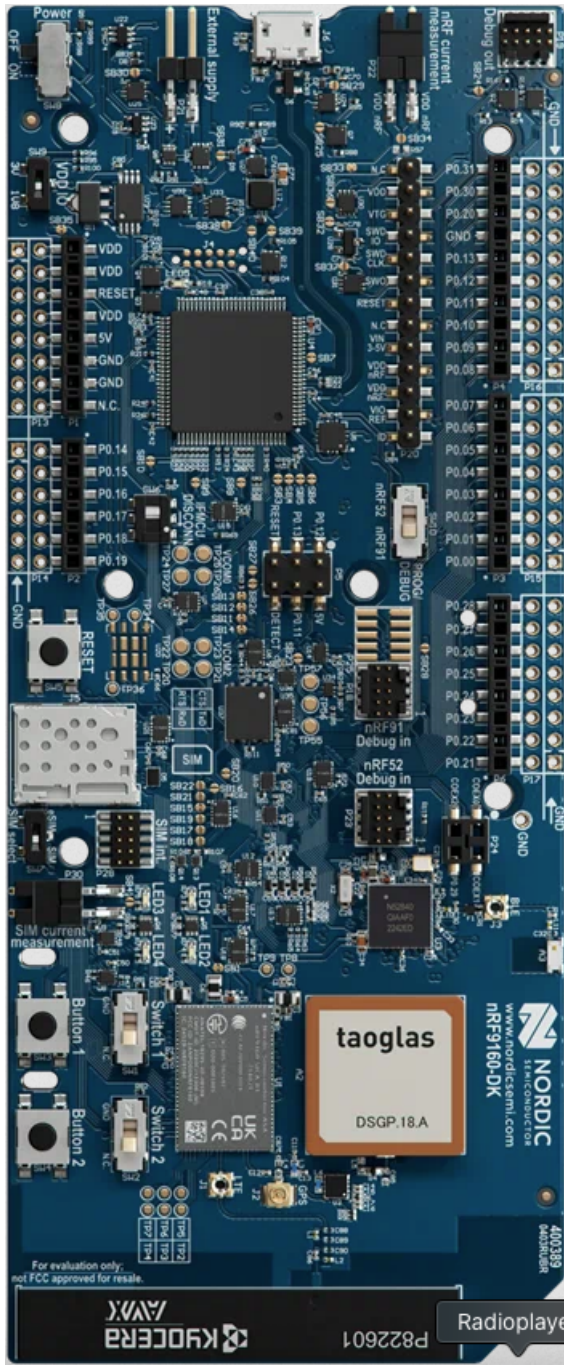


Figure 3.1: **nRF9160 Development Kit**

Nordic Semiconductor nRF9160 Development Kit showing the main circuit board with integrated cellular and GPS antennas, USB connector, and development interface pins.

Source: <http://www.nordicsemi.com/Products/Development-hardware/nRF9160-DK>

3.2.1 Operating System and SDK

The firmware for both experimental devices was based on the Zephyr Real-Time Operating System (RTOS) version 2.9.1. Zephyr is a lightweight, scalable, and modular RTOS designed for resource-constrained embedded systems. It offers support for Nordic Semiconductor hardware platforms. The primary motivation for its selection was its close integration with Nordic's development environment, along with its wide community and industrial support.

The project was developed using the nRF Connect Software Development Kit (SDK) (v2.9.1), which is the official SDK from Nordic Semiconductor built on top of Zephyr. The SDK offers a range of essential components, including device drivers, board support packages, protocol libraries, and example applications. The basis for this project was two Zephyr sample applications:

- `lwm2m_client`: used for the LWM2M implementation and extended to support sensor simulation and performance logging.
- `mqtt_simple`: used as a foundation for MQTT testing, including custom GNSS integration and performance metrics collection.

3.2.2 Development Environment

The development of the entire software was implemented through the use of Visual Studio Code on a macOS platform. Nordic's toolchain and dependencies were managed using the west meta-tool. The firmware was installed on the nRF9160 boards via USB, and debugging was managed using Universal Asynchronous Receiver-Transmitter (UART) logging mechanisms.

3.2.3 GNSS and AGNSS Integration

For GNSS positioning, the firmware included Assisted GNSS (AGNSS) functionality, which used Secure User Plane Location (SUPL) data from Google's SUPL server. This strategy leads to a reduction in time, which was found to be significant in low-power and cold-start scenarios, where it was critical to minimize the Time to First Fix (TTFF).

3.2.4 Communication Infrastructure

In this project, two separate IoT communication protocols were evaluated: The first is the MQTT protocol, and the second is the LWM2M protocol. The implementation of these systems was based on independent server infrastructures.

- **LwM2M Server:** The public *Eclipse Leshan* demo server was used to manage and observe the LWM2M client device. Communication occurred over DTLS with PSK authentication for encrypted transport.

- **MQTT Broker:** A private *Mosquitto* MQTT broker (version 2.0.11) was hosted on a local Raspberry Pi running in a home server setup. Secure communication was ensured using TLS with certificate-based authentication.

3.2.5 Data Storage and Backend Processing

Collected measurement data from both devices was stored in a PostgreSQL 15.10 database running on the same Raspberry Pi server as the MQTT broker. A custom Python (v3.12.9) application was developed to:

- Receive and parse messages from MQTT.
- Write telemetry and metadata to the PostgreSQL database.
- Aggregate, analyze, and visualize performance metrics across both technologies and protocols.

Python libraries such as `psycopg2`, `pandas`, and `matplotlib` were employed for data processing, visualization, and statistical comparison. The data aggregation from both boards is further detailed in Section 3.3.

3.2.6 Multi-Board Setup

Two separate nRF9160 Development Kits were used in parallel for the duration of the experiments. One device was dedicated to running the LWM2M client, while the other simultaneously executed the MQTT client application with GNSS tracking enabled. This dual-board configuration enabled synchronized and unbiased performance comparisons between the two protocol stacks under identical environmental and network conditions.

3.3 Measurement setup

To ensure extensive performance evaluation, both nRF9160 Development Kits were configured with UART-based logging capabilities. It has been determined that each board is equipped with a Virtual COM Port (VCOM) interface via USB, which provides three virtual serial ports. These include:

- **VCOM Port 0** was used for general application logging, including output from the main firmware (e.g., network statistics, GPS data, timing metrics).
- **VCOM Port 2** (the third port) was reserved for capturing raw modem traces, which consist of binary diagnostic data generated directly by the cellular modem.

The identification of each board was facilitated by its unique device ID, a feature that allowed the Python data acquisition scripts to dynamically assign the correct serial interfaces to the respective MQTT and LWM2M clients. Both development kits were connected to a macOS host system via a powered USB hub.

3.3.1 Firmware Workflow and Test Procedure

The firmware executed on each development kit was designed to emulate realistic application-layer traffic patterns while allowing precise control over network selection and data flow. The experiment was structured into three phases per device, executed in a controlled sequence to ensure comparable performance conditions.

3.3.1.0.1 MQTT and GNSS Board The board assigned to the MQTT workload followed a three-step operation pattern:

1. **GNSS Initialization and Fix Acquisition:** Upon boot, the firmware initiates a connection to the cellular network, choosing between LTE-M and NB-IoT based on the internal Zephyr network selection logic, which evaluates available signal quality and connection readiness. Once connected, the board requests SUPL assistance data over the active link to accelerate TTFF for the onboard GNSS module. The system then awaits a valid position fix. After that, the cellular connection is gracefully released.
2. **MQTT Uplink via LTE-M:** The firmware reconnects to the cellular network, this time explicitly selecting the LTE-M access technology. A fixed-size payload of 128 bytes is transmitted to a designated MQTT broker using MQTT version 3.1.1 with QoS level 0, which provides "at most once" delivery semantics. After transmission, the device disconnects from the network.
3. **MQTT Uplink via NB-IoT:** The same procedure is repeated, but the device connects via NB-IoT instead of LTE-M. The same 128-byte payload is transmitted to the MQTT broker using MQTT version 3.1.1 with QoS 0. Following this, the firmware stops execution.

This operational structure allowed for a direct comparison between LTE-M and NB-IoT uplink performance within the same environmental and hardware constraints, with GNSS serving as an additional performance parameter for initial fix acquisition under assisted conditions.

3.3.1.0.2 LwM2M Board The second board, used for LWM2M evaluation, executed a similar sequence, but with a distinct communication stack and use case:

- LwM2M Session over LTE-M:** The board establishes a cellular connection explicitly over LTE-M and connects to a remote LWM2M server. Upon successful registration, a local Python script running on the host system triggers a series of sample data reads via the LWM2M interface. Simultaneously, the script captures logs and modem traces. After a delay of 20 seconds to allow interaction and background communication, the board disconnects from the LTE-M network.
- LwM2M Session over NB-IoT:** The board reattaches to the network, this time using the NB-IoT radio access technology, and repeats the process: establishing a connection with the LWM2M server, enabling the Python script to perform the same read operations. After data collection, the firmware disconnects and stops execution.

By executing LWM2M communication on both LTE-M and NB-IoT sequentially within the same firmware cycle, the setup provides a direct comparison of end-to-end latency, registration time, and protocol responsiveness across both radio technologies.

3.3.2 Data Collection and Logging Framework

A custom Python 3.12 script was developed using the pyserial library to continuously monitor and log data from all active UART ports. The script simultaneously managed the two boards, extracting and timestamping performance metrics in real-time. The following parameters were logged:

- **Network Parameters:**
 - Network Mode (LTE-M or NB-IoT)
 - Access Point Name (APN)
 - Tracking Area Code (TAC)
 - Mobile Country Code (MCC) and Mobile Network Code (MNC)
 - Frequency Band and E-UTRA Absolute Radio Frequency Channel Number (EAR-FCN)
 - Cell ID and Physical Cell ID
 - Transmission Power, Repetition Counts (Tx/Rx), Coverage Enhancement (CE) level
 - eDRX cycle
 - Signal quality metrics: Reference Signal Received Power (RSRP), Reference Signal Received Quality (RSRQ), SNR, and Downlink (DL) Pathloss
 - Tracking Area Update (TAU) configuration and triggers
 - Link quality estimate and Energy Estimate

- **Connection Performance:**
 - Time required to attach to the cellular network
 - Time to establish a connection to the respective application-layer protocol (MQTT or LWM2M)
 - Basic uplink throughput metrics based on fixed-size UDP payloads
- **Geolocation Data:**
 - GPS coordinates retrieved from the MQTT-enabled device via GNSS logging

The parsing of this information was executed in real-time, and the resultant data was stored in a PostgreSQL 15.10 database that was located on the same Raspberry Pi server that was being used to operate the MQTT broker. This enabled efficient querying, post-processing, and data correlation across multiple experiments and geographic locations.

3.3.3 Modem Trace Analysis

To support the high-level logging, low-level modem traces were collected in parallel from both boards. The modem trace data, which was captured via the VCOM trace port, was converted from its binary format into industry-standard .pcapng files using Nordic's nrfutil trace tool. These files allow for detailed packet-level inspection using Wireshark or programmatic analysis with the pyshark library.

Despite not being stored directly in the database due to their size and complexity, the .pcapng traces were archived and subsequently analyzed during the evaluation phase. This analysis was used to validate observed performance anomalies, retransmissions, and protocol behavior under different network conditions.

3.3.4 Parallelized Testing

During the experimental phase, both boards were operated in parallel. The LWM2M client was executed on one device, while the second board simultaneously ran the MQTT client with GNSS functionality. This parallelized approach ensured synchronized measurement conditions across both protocols and cellular technologies, thus minimizing temporal and environmental biases in the collected performance data.

3.4 Challenges

A number of technical and methodological challenges were encountered during the implementation and evaluation phases of this project, particularly in the areas of low-level data acquisition, protocol trace analysis, and automation of the measurement framework.

3.4.1 Modem Trace Extraction and Analysis

A notable challenge was the extraction and interpretation of modem trace data from the nRF9160 development boards. These traces, which consist of raw binary logs generated by the cellular modem, are essential for undertaking a detailed analysis of protocol behavior and network-layer interactions. However, the process of converting these binary files into a human-readable format proved to be non-trivial.

At the beginning, the documentation provided minimal guidance on the interpretation and decoding of modem trace files. After a detailed investigation, the `nrfutil trace` utility was identified as the appropriate tool for converting the binary logs into the industry-standard `.pcapng` format, which can be analyzed using Wireshark. After conversion, the interpretation of the trace content required a significant investment of time and effort due to two factors. Firstly, there was a lack of detailed documentation, which made it difficult to understand the data. Secondly, the number of packets per session was extremely high, which further complicated the analysis. The process of identifying relevant protocol messages (e.g., attach requests, handovers, retransmissions) within extensive and frequently noisy traces proved to be a manual effort of significant duration.

3.4.2 Throughput Measurement Implementation

Another technical challenge encountered was the implementation of a basic throughput measurement over the raw cellular link using UDP. Link throughput was measured using a UDP-based uplink speed test, where the device transmitted a 512-byte payload to a remote server. The server calculated immediate throughput by measuring the time difference between packet arrivals using precise kernel timestamps, accounting for all protocol headers (UDP, Internet Protocol (IP), Ethernet). This metric represents the effective uplink data rate achievable under current radio frequency conditions.

The measurement approach employed a two-packet timing method: the client first sends a 1-byte trigger message followed immediately by the 512-byte data payload. The server captures nanosecond-precision timestamps for both packets and calculates throughput based on the second packet's total size (554 bytes including headers) divided by the inter-packet arrival time. In consideration of the constrained nature of the embedded environment and the limitations of the underlying network stack, close attention was required to ensure optimal performance metrics, including packet sizing, buffering, and timing accuracy.

This approach was implemented to ensure the reliability and reproducibility of the experimental results, providing a standardized measurement of immediate uplink throughput rather than theoretical link capacity. This was crucial during the testing phase under NB-IoT conditions, where constrained bandwidth and high latency can readily introduce distortions in performance metrics, requiring precise timing measurements to accurately capture the effective data transmission capabilities.

3.4.3 Measurement Framework Stability and Automation

The establishment of a reliable and reproducible measurement configuration was found to be a time-consuming process. The objective of the study was to collect a wide range of performance metrics (e.g., signal strength, connection time, GPS location, throughput) across two parallel devices in a consistent and synchronized manner. The successful integration of these components, which included UART logging, modem trace conversion, GPS data capture, protocol-level timing, and database storage, was essential for the achievement of this objective. Ensuring that the setup was sufficiently robust to operate autonomously for extended periods and under varying network conditions presented additional challenges. To ensure the accuracy and reliability of the data, multiple iterations were necessary to refine the Python-based logging and aggregation scripts, address serial port conflicts, and manage edge cases such as dropped connections or incomplete logs.

4. Measurements

The measurements produced a total of 312 datasets, including 156 datasets for the MQTT protocol and 156 datasets for the LWM2M protocol. Each dataset contains 27 parameters, which were obtained directly from the nRF9160 development board. Furthermore, for each dataset, there is a corresponding pcapng file that stores modem information, resulting in a total of 312 pcapng modem traces. The measurements were conducted in 156 different locations within the Cologne area, as illustrated in Figure 4.1.

Protocol-Specific Metrics from PCAP Analysis

The following parameters were extracted from modem trace files converted to Packet Capture (PCAP) format and analyzed using pyshark. These metrics provide insights into low-level protocol behavior and network interaction patterns.

- **Retransmissions**

[count]

Number of packet retransmissions observed during a communication session. The calculation method varies by protocol:

MQTT (TCP-based): Retransmissions are detected by analyzing TCP sequence numbers and acknowledgment patterns on port 8883. The analysis tracks outgoing packets with their sequence numbers and matches them with incoming acknowledgments. Retransmissions are identified when duplicate sequence numbers appear or when acknowledgments arrive out of order, indicating that packets were lost and required retransmission by the TCP protocol stack.

LWM2M (UDP-based): Since UDP is connectionless, retransmissions must be detected at the application layer through CoAP request-response pairing. The analysis automatically detects LWM2M communication ports (typically 5683, 5684, 5000, 8000) and tracks outgoing CoAP requests. Retransmissions are counted when requests are sent without corresponding responses within reasonable timeout periods, indicating that the CoAP confirmable message mechanism triggered retransmission due to lost or delayed packets.

- **Latency**

[s]

End-to-end latency measured differently for each protocol based on their underlying transport mechanisms:

MQTT Latency Calculation: Measured by analyzing TCP acknowledgment timing for packets on port 8883. The analysis tracks the time difference between when a TCP

Measurement Locations



Figure 4.1: Data Collection Locations

The figure shows the distribution of the 156 measurement locations. Each marker represents a single conducted measurement.

segment is transmitted and when its corresponding acknowledgment is received. This provides insight into the round-trip time for MQTT communication, filtered to include only realistic latency values between 0-5 seconds to exclude measurement artifacts and packet reordering effects.

LWM2M Latency Calculation: Based on CoAP request-response timing patterns. The analysis measures the time between outgoing CoAP requests to LWM2M servers and their corresponding responses. This application-layer latency measurement captures the end-to-end responsiveness of the LWM2M protocol, with filtering applied to include only response times between 0-10 seconds to account for the potentially higher latency characteristics of constrained networks.

- **Security Handshake Time**

[s]

Time required to complete the security establishment phase for encrypted connections:

MQTT TLS Handshake: Detected through analysis of TCP payload sizes and patterns on port 8883. The analysis identifies TLS handshake phases by examining payload characteristics: small initial packets (20-50 bytes) indicate Client Hello messages, large subsequent packets (>100 bytes) suggest Server Hello and certificate exchange, followed by key exchange and finished messages. The handshake duration is measured from the first TLS packet to the completion of the certificate exchange phase.

TLS Handshake Phases Detected:

1. Client Hello (small payload 20-50 bytes)
2. Server Hello + Certificate (large payload >100 bytes)
3. Key Exchange (medium payload)
4. Finished Messages (small payload)

LWM2M DTLS Handshake: Employs similar heuristic approaches applied to UDP traffic on LWM2M ports, though DTLS detection presents additional challenges due to UDP's connectionless nature. The analysis identifies DTLS handshake patterns by examining packet sizes and timing patterns characteristic of DTLS certificate exchange and key establishment procedures.

- **RRC State Changes**

[count]

Number of Radio Resource Control state transitions observed during a communication session. These are extracted from AT command responses embedded in the PCAP trace data. The analysis monitors for specific AT command indicators that signal RRC state transitions, particularly focusing on connection establishment and release events.

CSCON Status Codes [18]:

- +CSCON: 0 = RRC Idle (radio connection released)

- +CSCON: 1 = RRC Connected (radio connection active)

Frequent RRC state changes impact energy consumption and connection stability, especially relevant for battery-powered outdoor sensors.

- **Network Registration Changes**

[count]

Number of network registration state changes occurring during a communication session. Extracted by monitoring Non-Access Stratum (NAS) (Non-Access Stratum) signaling messages captured in the modem trace data. The analysis tracks changes in network registration status by parsing AT command responses that indicate registration state transitions.

CEREG Status Codes [17]:

- +CEREG: 0 = Not registered, not searching
- +CEREG: 1 = Registered, home network
- +CEREG: 2 = Not registered, searching
- +CEREG: 3 = Registration denied
- +CEREG: 4 = Unknown
- +CEREG: 5 = Registered, roaming

High values suggest network instability or mobility-related issues that could affect outdoor sensor reliability and indicate potential connectivity problems during deployment.

Data Processing and Filtering

The PCAP analysis implements several filtering mechanisms to ensure data quality:

Latency Filtering:

- MQTT latencies outside 0-5000ms range are excluded
- LWM2M response times outside 0-10000ms range are excluded
- Filters eliminate unrealistic values caused by packet reordering

Signal Quality Filtering:

- AT command values of 255 are treated as invalid measurements
- Empty or malformed AT responses are ignored
- Only complete measurement sequences are included in analysis

Session Boundary Detection:

- Sessions are automatically split based on AT%SYSTEMMODE commands
- Protocol-specific port detection enables accurate traffic classification
- Incomplete sessions without clear boundaries may result in partial analysis

These parameters form the basis for evaluating cellular link reliability, protocol responsiveness, and deployment-specific performance characteristics across communication technologies and protocol layers. The combination of modem Application Programming Interface (API) data, custom timing measurements, and PCAP trace analysis provides comprehensive visibility into both radio-level and protocol-level performance characteristics essential for outdoor deployment planning.

4.1 Data Processing and Analysis Methodology

The collected measurement data was processed and analyzed using Python 3.12. A custom analysis pipeline was developed to extract metrics, generate visualizations, and enable comparative evaluations across different communication technologies and application protocols.

Software Stack and Libraries

The following Python libraries were used during the measurement collection and analysis:

- `pyserial`: for serial communication with nRF9160 development kits and AT command interface
- `paho-mqtt`: for MQTT client implementation and protocol testing
- `pyshark`: for PCAP file analysis and network packet inspection
- `scapy`: for packet capture and network traffic analysis
- `pandas`, `numpy`: for numerical operations, statistical analysis, and structured data processing
- `scipy.stats`: for statistical testing including Mann-Whitney U tests and Kruskal-Wallis analysis
- `matplotlib.pyplot`, `seaborn`: for static 2D visualizations, including boxplots and statistical plots

- `json`, `os`: for handling configuration files, data storage, and directory traversal
- `requests`: for HTTP-based communication and server interactions
- `threading`, `queue`: for concurrent measurement execution and data collection

All measurement logs were stored in structured formats (JSON and PCAPNG), parsed using specialized libraries, and analyzed in Jupyter Notebooks and standalone Python scripts for full performance evaluation.

Visualization and Statistical Methods

The following visual and statistical techniques were used to present and explore the measurement data:

- **Confidence Interval Plots:** These plots display the mean value of a metric along with its confidence interval, providing insight into the statistical reliability and variability of the measurements. For a given confidence level α (typically 95%), the confidence interval for the population mean μ is calculated as [10]:

$$CI = \bar{x} \pm t_{\alpha/2,n-1} \cdot \frac{s}{\sqrt{n}}$$

where:

- \bar{x} is the sample mean
- $t_{\alpha/2,n-1}$ is the critical value from the t-distribution with $n - 1$ degrees of freedom
- s is the sample standard deviation
- n is the sample size

The confidence interval represents the range within which the true population mean is likely to fall with the specified confidence level. These plots are valuable for comparing performance metrics between different protocol-technology combinations while accounting for measurement uncertainty.

Statistical significance testing in confidence interval plots: To determine whether observed differences between groups are statistically significant, hypothesis testing is performed beside the confidence interval visualization. The choice of statistical test depends on the number of groups being compared:

Mann-Whitney U Test: A non-parametric statistical test used for comparing two independent groups (e.g., NB-IoT vs. LTE-M) [16]. This test is suitable when data does

not meet the assumptions of parametric tests (normality, equal variances). The Mann-Whitney U test checks whether one group tends to have larger values than the other by ranking all observations and comparing rank sums between groups.

Kruskal-Wallis Test: A non-parametric statistical test used when comparing multiple independent groups (e.g., all four protocol-technology combinations: MQTT+NB-IoT, MQTT+LTE-M, LWM2M+NB-IoT, LWM2M+LTE-M) [15]. This test extends the Mann-Whitney U test to more than two groups and checks whether the median values differ significantly across groups. The test statistic H is calculated as:

$$H = \frac{12}{N(N+1)} \sum_{i=1}^k \frac{R_i^2}{n_i} - 3(N+1)$$

where:

- k is the number of groups being compared
- N is the total number of observations across all groups
- n_i is the number of observations in group i
- R_i is the sum of ranks for group i

p-value interpretation: The p-value represents the probability of observing the measured difference (or a more extreme difference) between groups, assuming the null hypothesis (no difference between groups) is true [12]. Conventional interpretation levels are:

- $p < 0.001$: Highly significant (***) - very strong evidence against the null hypothesis
- $p < 0.01$: Significant (**) - strong evidence against the null hypothesis
- $p < 0.05$: Significant (*) - moderate evidence against the null hypothesis
- $p \geq 0.05$: Not significant (ns) - insufficient evidence to reject the null hypothesis

These statistical tests ensure objective determination of whether observed performance differences between groups are statistically meaningful rather than due to random variation. The Mann-Whitney U test is used for two-group comparisons (technology comparisons), while the Kruskal-Wallis test is used for multi-group comparisons (protocol-technology combination analysis).

- **Kernel Density Estimation (KDE):** A non-parametric statistical method used to estimate the probability density function of a continuous random variable from a finite dataset [11]. Unlike histograms, Kernel Density Estimation (KDE) provides a smooth, continuous estimate of the underlying distribution. The KDE estimator is defined as:

$$\hat{f}_h(x) = \frac{1}{nh} \sum_{i=1}^n K\left(\frac{x - x_i}{h}\right)$$

where:

- $\hat{f}_h(x)$ is the estimated density at point x
- n is the number of data points
- h is the bandwidth (smoothing parameter)
- $K(\cdot)$ is the kernel function
- x_i are the observed data points

In this thesis, a Gaussian kernel is employed for all KDE visualizations, where the kernel function becomes:

$$K(u) = \frac{1}{\sqrt{2\pi}} e^{-\frac{u^2}{2}}$$

The bandwidth h controls the smoothness of the estimate: smaller values produce more detailed curves but may overfit to noise, while larger values create smoother curves but may result in a loss of important features. KDE plots provide detailed insight into the shape, modality, and skewness of data distributions, making them ideal for comparing performance characteristics between NB-IoT and LTE-M technologies or across different protocol-technology combinations.

- **Geolocation-based Measurement Point Visualization:** Simple geographic visualization of measurement locations generated using the `folium` Python library, which provides an interface to the Leaflet.js mapping library. These maps display the spatial distribution of measurement points across the geographic area where data collection was conducted. The maps utilize reliable tile layer sources:

- **OpenStreetMap:** The primary map data source, providing detailed street-level information and geographic features. OpenStreetMap is a collaborative, open-source mapping project that provides free geographic data worldwide.
- **CartoDB:** Additional tile layers (Positron) from CartoDB/CARTO, offering light grayscale styling for clear visualization of measurement points.

The visualization displays:

- **Measurement locations:** Individual data collection points displayed as red circular markers
- **Geographic context:** Street names and geographic features to provide spatial reference for the measurement campaign

- **Coverage area:** Visual representation of the geographic extent of the measurement study

This geographic visualization enables analysis of measurement distribution and provides context for understanding the environmental conditions under which the performance evaluations were conducted.

This analysis framework allowed the efficient processing of large measurement datasets and the generation of consistent, high-quality visual outputs for comparison between NB-IoT and LTE-M, as well as across all protocol-technology combinations.

4.2 Measurement Results

This section presents the empirical results obtained from the measurement campaign performed across multiple geographic locations. The analysis is structured into two complementary sections: the first analyzed performance characteristics and differences between the two cellular communication technologies (NB-IoT and LTE-M), while the second evaluates the behavior of application protocols (MQTT and LWM2M) across both communication technologies. Figure 4.1 illustrates the spatial distribution of measurement locations, providing geographic context for the data collection campaign.

4.2.1 Communication Technology comparisons

This subsection presents a systematic comparison of NB-IoT and LTE-M technologies across multiple radio frequency and performance parameters. The analysis includes signal quality metrics, power consumption characteristics, and connection performance indicators.

Transmit Power Analysis

Figure 4.2 presents the transmit power distribution analysis using kernel density estimation and confidence interval visualization. The data reveals that LTE-M exhibits a mean transmit power approximately 3 dBm higher than NB-IoT, with largely overlapping distributions between the two technologies. Both technologies demonstrate similar variance characteristics in their power distributions. Statistical analysis using the Mann-Whitney U test yields a p-value of 0.0039, providing strong evidence for a statistically significant difference in transmit power requirements between the technologies.

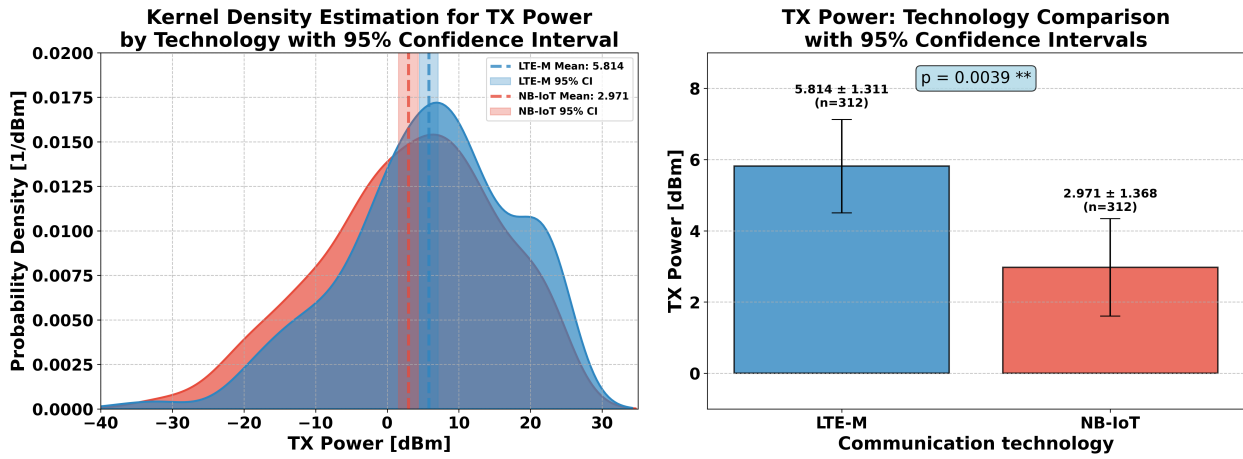


Figure 4.2: TX Power Distribution

The figure shows the transmit power distribution for NB-IoT and LTE-M technologies. Lower TX power indicates better energy efficiency and coverage conditions.

RSRP Analysis

The RSRP measurements, visualized in Figure 4.3 through KDE and confidence interval plots, demonstrate that NB-IoT achieves a mean RSRP approximately 6 dBm higher than LTE-M. Both technologies exhibit comparable variance in their RSRP distributions. The statistical analysis using the Mann-Whitney U test returns a p-value of $p < 0.001$, indicating highly significant evidence that NB-IoT consistently receives stronger reference signal power compared to LTE-M under the measured conditions.

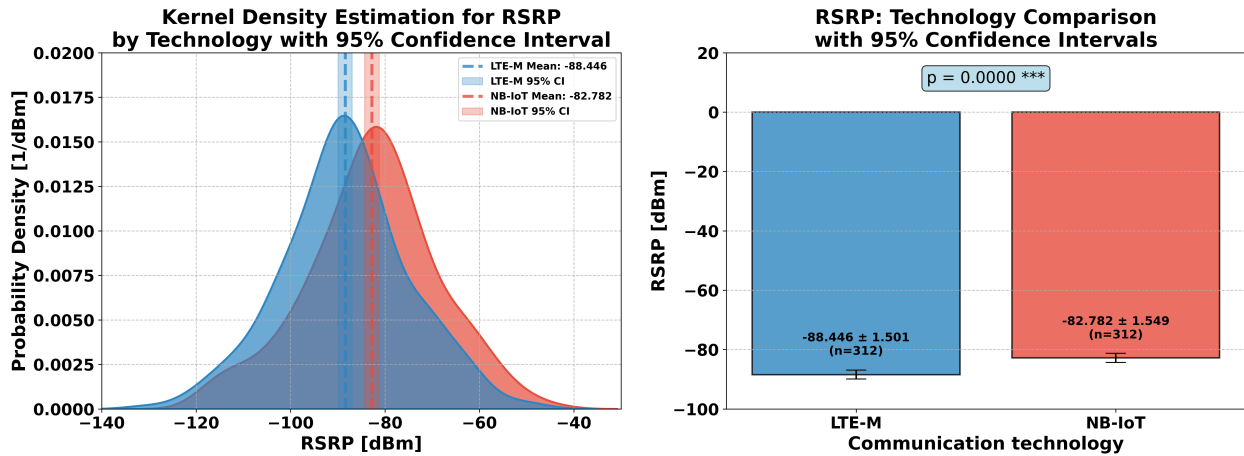


Figure 4.3: **RSRP Distribution**

The figure shows RSRP values measured across different locations. Higher RSRP values indicate better signal coverage and link quality.

RSRQ Analysis

Figure 4.4 illustrates the RSRQ distribution comparison, showing that NB-IoT maintains a mean RSRQ approximately 3.5 dB higher than LTE-M. Notably, LTE-M showed greater variance in RSRQ measurements compared to NB-IoT, suggesting more variable signal quality conditions. The Mann-Whitney U test produces a p-value of $p < 0.001$, providing highly significant evidence that NB-IoT delivers superior reference signal quality under the evaluated deployment scenarios.

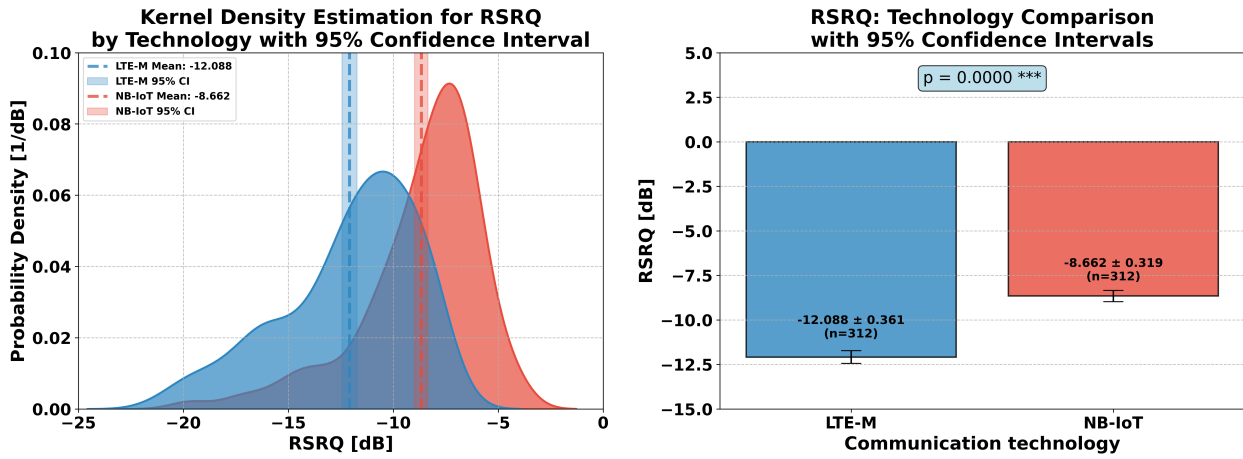


Figure 4.4: **RSRQ Distribution**

The figure shows RSRQ measurements comparing NB-IoT and LTE-M signal quality. RSRQ reflects the quality of the received reference signal.

SNR Analysis

The SNR distribution analysis, presented in Figure 4.5, reveals that NB-IoT achieves a mean SNR approximately 3 dB higher than LTE-M. NB-IoT demonstrates greater variance in SNR measurements compared to LTE-M. Statistical testing using the Mann-Whitney U test yields a p-value of $p < 0.001$, providing highly significant evidence of superior signal-to-noise performance for NB-IoT technology across the measurement campaign.

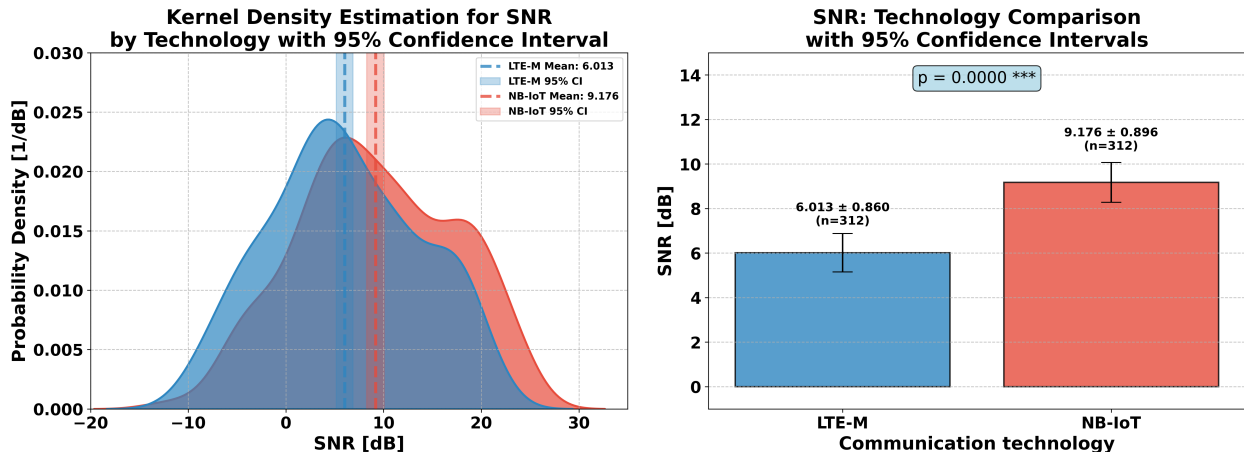


Figure 4.5: **SNR Distribution**

The figure shows SNR measurements for both technologies. Higher SNR values indicate better signal quality and more reliable communication.

Connection Time Analysis

Figure 4.6 presents the cellular network connection establishment time analysis. The data shows that NB-IoT requires approximately 6.3 seconds longer for network attachment compared to LTE-M. LTE-M demonstrates essential lower variance in connection times, indicating more consistent connection establishment behavior. Statistical analysis using the Mann-Whitney U test confirms highly significant differences ($p < 0.001$) between the technologies. The presence of outliers, particularly evident in NB-IoT measurements, contributes to the observed higher variance in connection time distributions.

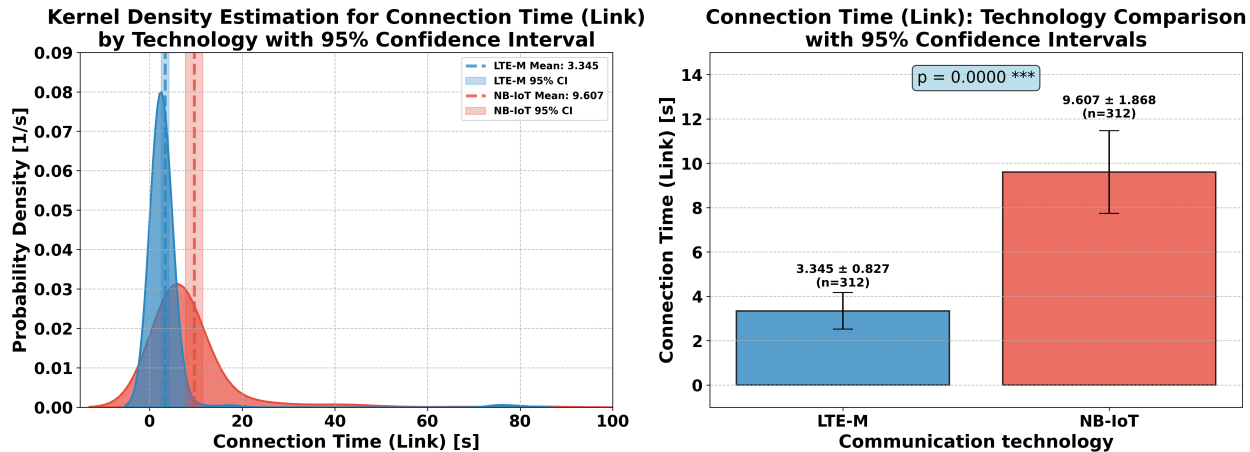


Figure 4.6: **Link Connection Time Distribution**

The figure shows the time required to establish cellular network connectivity. Lower connection times indicate faster network attachment and improved user experience.

Downlink Pathloss Characteristics

The downlink pathloss analysis, shown in Figure 4.7, shows minimal differences between technologies. NB-IoT exhibits a mean pathloss 0.4 dB lower than LTE-M, with both technologies demonstrating very similar variance characteristics. The Mann-Whitney U test produces a p-value of 0.608, indicating no statistically significant evidence of pathloss differences between NB-IoT and LTE-M under the measured conditions.

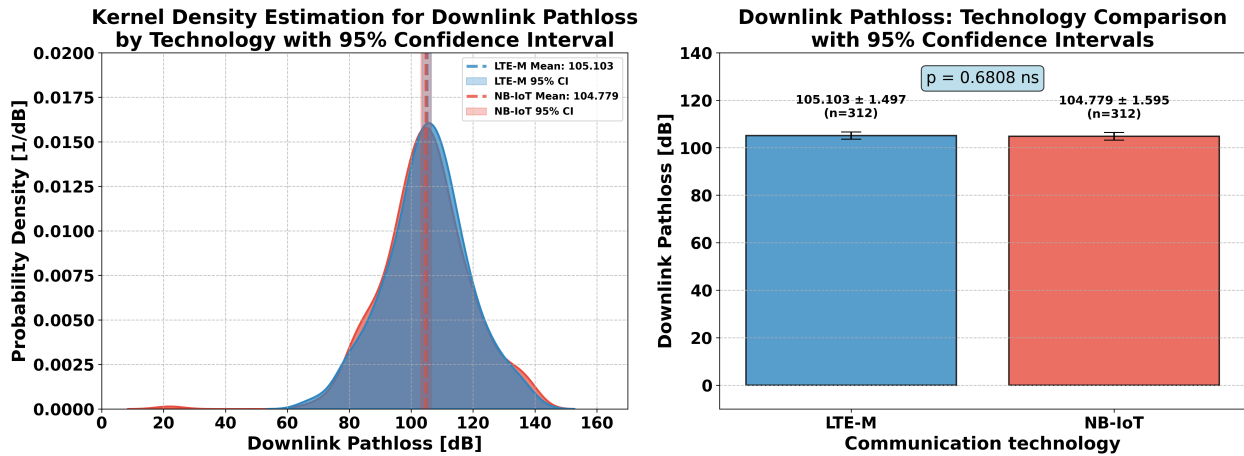


Figure 4.7: **Downlink Pathloss Distribution**

The figure shows signal attenuation in the downlink path for both NB-IoT and LTE-M. Lower pathloss values indicate better propagation conditions.

Energy Consumption Estimates

Figure 4.8 presents the energy consumption estimate distributions, revealing that NB-IoT shows a mean energy estimate 0.3 units higher than LTE-M. Both technologies have similar variance characteristics. Statistical analysis using the Mann-Whitney U test yields a p-value of 0.0017, providing strong evidence of significant differences in relative energy consumption between the technologies. A notable characteristic observed in both distributions is the discrete pattern with three distinct peaks, reflecting the categorical nature of the energy estimate parameter, which is encoded as discrete integer values by the modem rather than continuous measurements. The observed distribution pattern indicates that both technologies predominantly operate within three specific energy consumption classes, likely corresponding to different coverage enhancement levels or network optimization states implemented by the cellular operator.

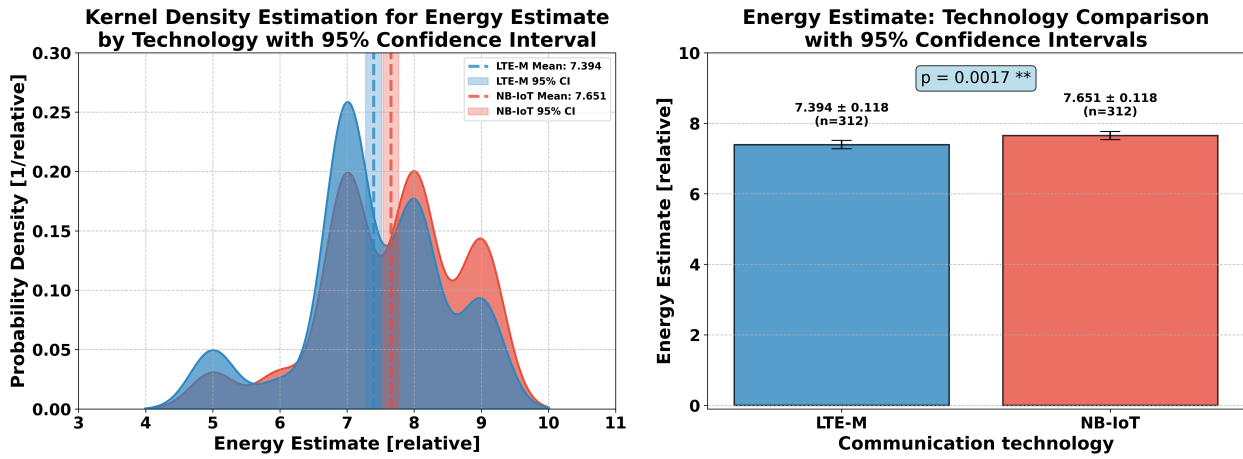


Figure 4.8: Energy Estimate Distribution

The figure shows relative energy consumption estimates for data transmission. Lower values indicate more energy-efficient communication.

Receive Repetitions Analysis

The receive repetitions analysis, shown in Figure 4.9, indicates that NB-IoT requires 0.3 counts fewer receive repetitions than LTE-M on average. LTE-M demonstrates higher variance in repetition requirements compared to NB-IoT. The Mann-Whitney U test produces a p-value of 0.25, indicating insufficient evidence to conclude significant differences in receive repetition requirements between the technologies.

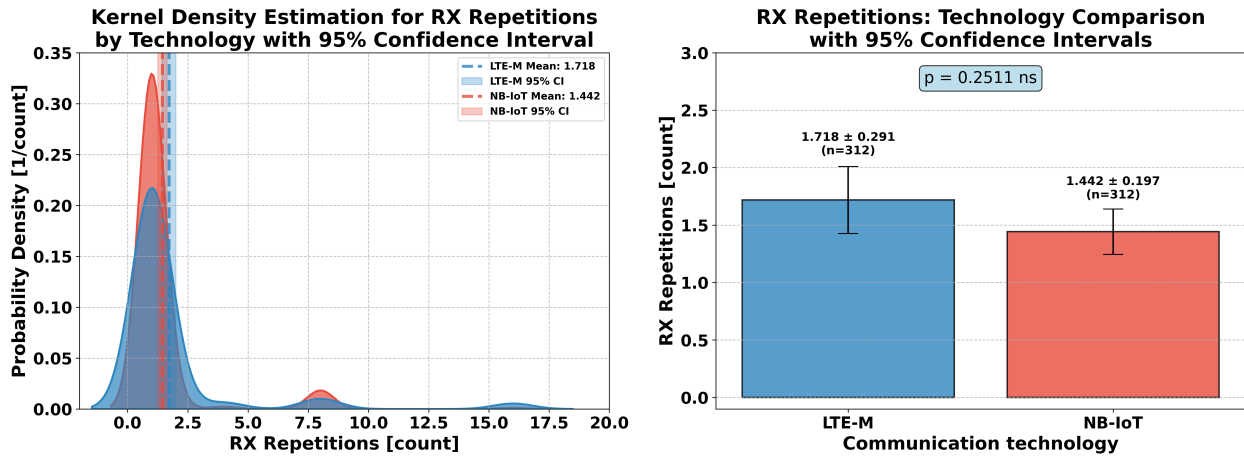


Figure 4.9: RX Repetitions Distribution

The figure shows the number of receive repetitions required for reliable communication. Higher repetitions indicate poorer link conditions.

Transmit Repetitions Analysis

Figure 4.10 presents the transmit repetitions comparison, showing that NB-IoT requires approximately 0.6 counts more transmit repetitions than LTE-M on average. NB-IoT exhibits greater variance and the presence of outliers in transmission repetition requirements. Statistical analysis using the Mann-Whitney U test yields a p-value of $p < 0.001$, providing highly significant evidence that NB-IoT requires more transmission repetitions for reliable uplink communication compared to LTE-M.

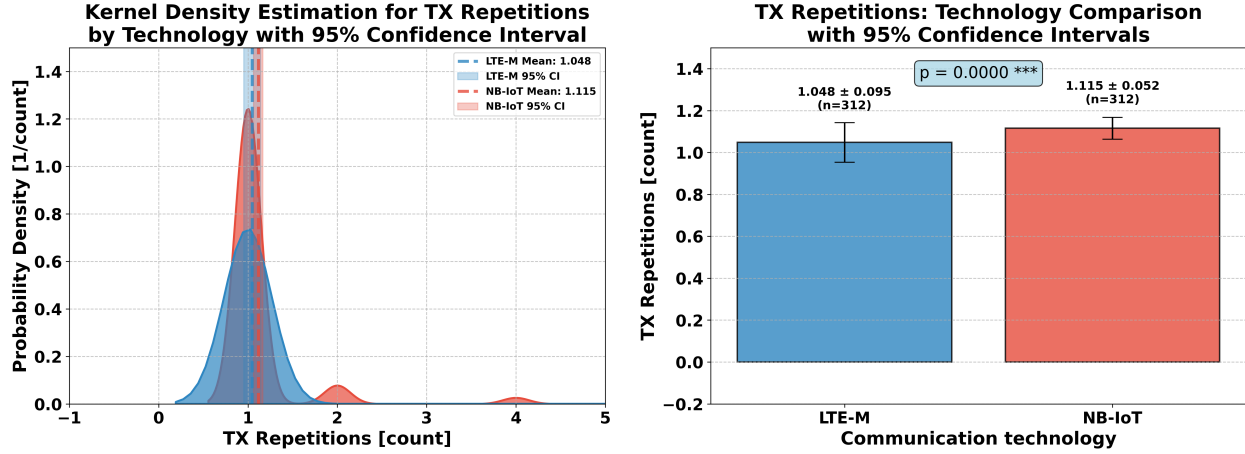


Figure 4.10: TX Repetitions Distribution

The figure shows the number of transmission repetitions required for reliable uplink communication. Higher repetitions indicate coverage enhancement needs.

Link Throughput Performance

The uplink throughput analysis, presented in Figure 4.11, reveals substantial differences between technologies. The measurement employed a UDP-based two-packet timing method where the device transmitted a 512-byte payload to a remote server, with throughput calculated based on precise kernel timestamps and total packet size including protocol headers (554 bytes total). NB-IoT achieves approximately 215 kbps lower uplink throughput than LTE-M on average. LTE-M demonstrates significantly higher variance in uplink throughput measurements. Statistical testing using the Mann-Whitney U test confirms highly significant differences ($p < 0.001$) between the technologies. The uplink data shows NB-IoT throughput consistently ranges between 0-100 kbps, while LTE-M has a peak around 300 kbps with a broad uplink distribution spanning 100-380 kbps. These uplink throughput characteristics directly impact the data transmission capabilities for outdoor sensor deployments, where sensor data must be efficiently transmitted from field devices to remote monitoring systems.

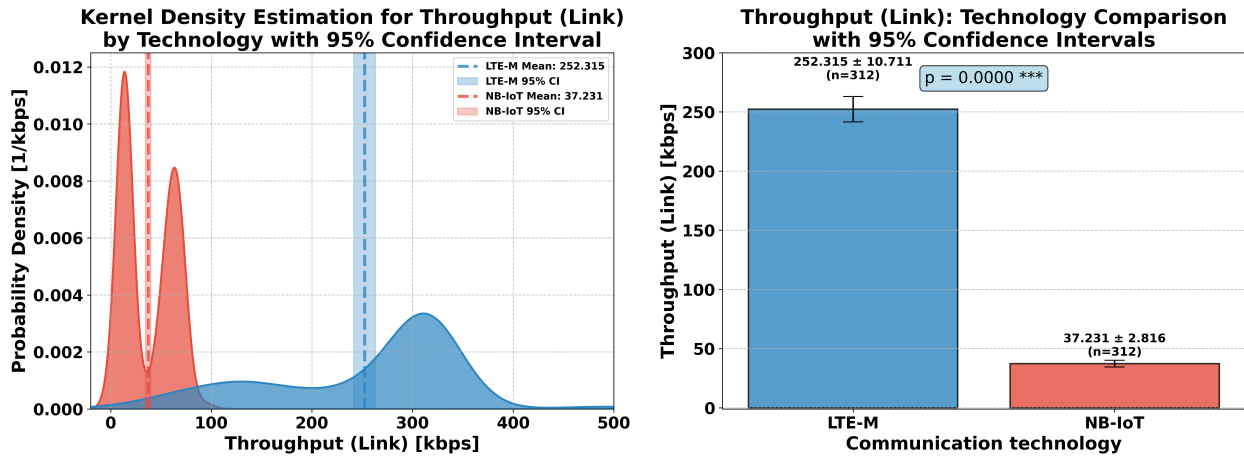


Figure 4.11: Link Throughput Distribution

The figure shows achieved data throughput for NB-IoT and LTE-M connections. Higher throughput values indicate better data transmission performance.

Uplink Frequency Analysis

Figure 4.12 illustrates the uplink frequency distribution, showing that LTE-M operates across two primary frequency bands: Band 20 (832-862 MHz) and Band 3 (1710-1785 MHz). NB-IoT utilizes Band 8 (880-915 MHz) and Band 20 (832-862 MHz). NB-IoT demonstrates lower variance in frequency utilization compared to LTE-M, indicating more constrained frequency band deployment. Both technologies share Band 20 for uplink transmission, while LTE-M additionally utilizes the higher frequency Band 3 and NB-IoT uses Band 8.

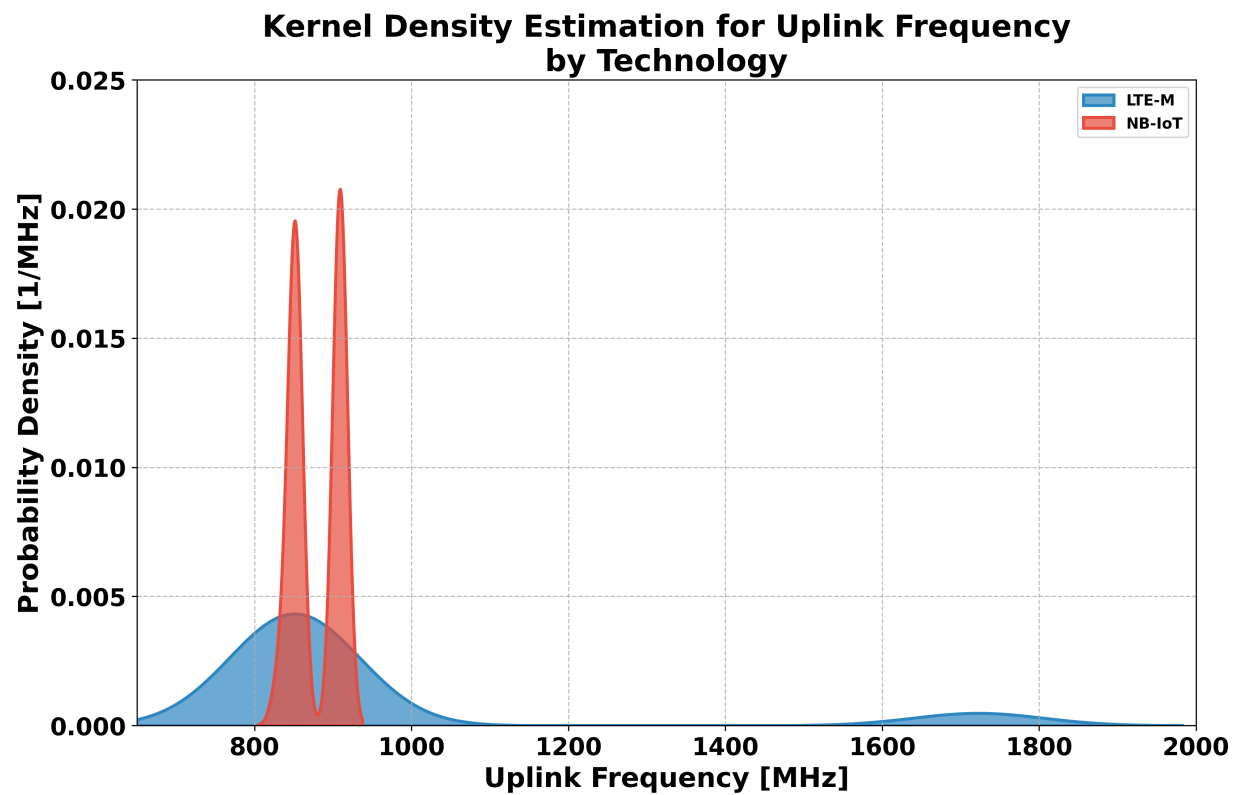


Figure 4.12: **Uplink Frequency Distribution**

The figure shows the uplink frequencies used for NB-IoT and LTE-M connections. Frequencies are derived from EARFCN values and reflect the radio access technology used.

Downlink Frequency Analysis

The downlink frequency analysis, shown in Figure 4.13, reveals that LTE-M operates on Band 20 (791-821 MHz) and Band 3 (1805-1880 MHz) for downlink transmission. NB-IoT utilizes Band 8 (925-960 MHz) and Band 20 (791-821 MHz) for downlink. Similar to uplink patterns, NB-IoT exhibits lower variance in downlink frequency usage compared to LTE-M, with both technologies sharing the lower frequency Band 20 while using different additional bands.

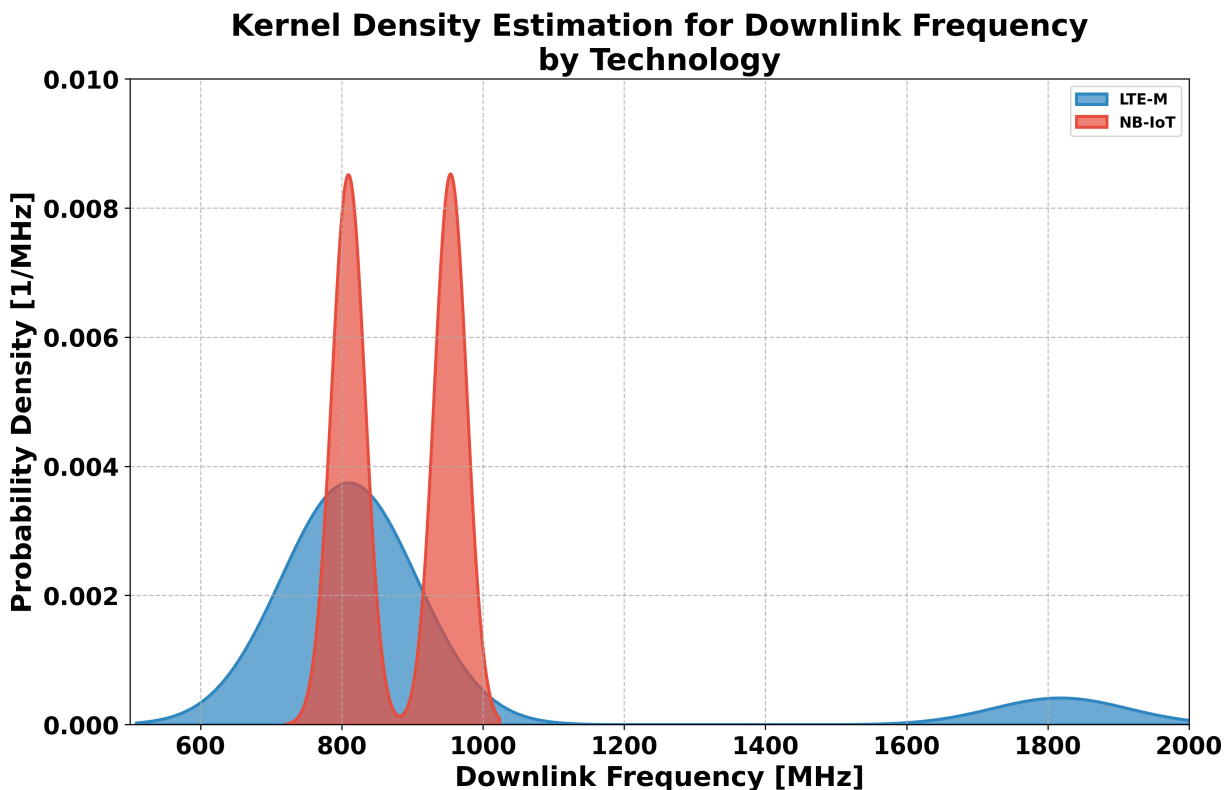


Figure 4.13: **Downlink Frequency Distribution**

The figure shows the downlink frequencies used for NB-IoT and LTE-M connections. Frequencies are derived from EARFCN values and reflect the radio access technology used.

Technology Radar Comparison

Figure 4.14 provides a multi-dimensional radar chart comparison of NB-IoT and LTE-M performance across normalized metrics. The visualization enables simultaneous assessment of multiple performance indicators, with values normalized to ensure cross-metric comparability and outlier suppression. The radar chart reveals that while some metrics such as transmit

repetitions and downlink pathloss show relatively similar performance between technologies, others including throughput, connection time, RSRQ, SNR, and RSRP demonstrate substantial differences.

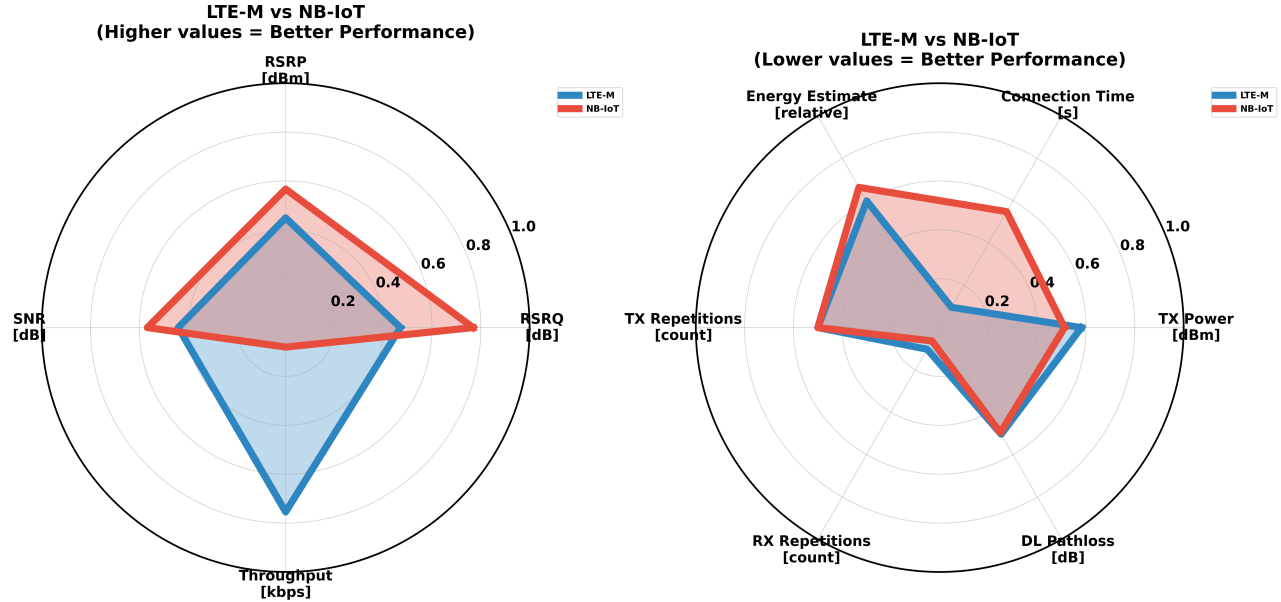


Figure 4.14: **Technology Comparison Radar Chart**

The figure provides a multi-dimensional comparison of NB-IoT and LTE-M across various performance metrics. The left radar chart shows metrics where higher values indicate better performance, while the right radar chart shows metrics where lower values indicate better performance.

Figure 4.15 presents a categorical performance summary highlighting the relative strengths of each technology across key performance indicators. The visualization identifies areas where NB-IoT demonstrates superior performance (including transmit power efficiency, RSRP, RSRQ, and SNR) versus areas where LTE-M dominates (including connection time, throughput, and transmission repetitions).

The communication technology comparison reveals performance characteristics for each technology. NB-IoT demonstrates superior signal quality metrics (RSRP, RSRQ, SNR) and energy efficiency, while LTE-M provides faster connection establishment and significantly higher data throughput capabilities. These findings build the foundation for protocol-specific performance analysis in the following subsection.

NB-IoT vs LTE-M Comparison

Metric	NB-IoT	LTE-M	Winner	Key Insight
TX power [dBm]	2.97±12.28 (n=312)	5.81±11.76 (n=312)	NB-IoT	Energy efficiency vs coverage
RSRP [dBm]	-82.78±13.91 (n=312)	-88.45±13.48 (n=312)	NB-IoT	Signal strength & coverage
RSRQ [dB]	-8.66±2.86 (n=312)	-12.09±3.24 (n=312)	NB-IoT	Signal quality & interference
SNR [dB]	9.18±8.04 (n=312)	6.01±7.72 (n=312)	NB-IoT	Noise immunity & robustness
Connection time (link) [s]	9.61±16.77 (n=312)	3.34±7.43 (n=312)	LTE-M	Network responsiveness
Throughput (link) [kbps]	37.23±25.28 (n=312)	252.31±96.15 (n=312)	LTE-M	Data transmission speed

Figure 4.15: Communication Technology Comparison Summary

The figure summarizes the performance differences between NB-IoT and LTE-M across key metrics. It highlights the strengths and weaknesses of each technology in terms of signal quality, connection time, and energy efficiency.

4.2.2 Protocol and Technology Combination Analysis

This subsection shows the performance characteristics of MQTT and LWM2M protocols operating across both NB-IoT and LTE-M technologies, resulting in four protocol-technology combinations. The analysis focuses on connection establishment, security handshake procedures, end-to-end latency, and network behavior metrics.

Connection Time Distribution

Figure 4.16 presents the full connection time analysis across all four protocol-technology combinations. The upper plot shows the kernel density estimation revealing the distribution characteristics, while the lower plot provides confidence interval comparison of mean values. The results show that MQTT over LTE-M achieves the fastest connection establishment with a mean time of 2.771 seconds, while MQTT over NB-IoT requires the longest connection time with a mean of 6.518 seconds. The Kruskal-Wallis test shows a p-value of $p < 0.001$, providing highly significant evidence of connection time differences across the combinations. The KDE visualization reveals that MQTT over NB-IoT and LWM2M over LTE-M exhibit substantially higher variance in connection times compared to the other combinations, which is confirmed by the confidence interval analysis showing broader uncertainty ranges for these combinations.

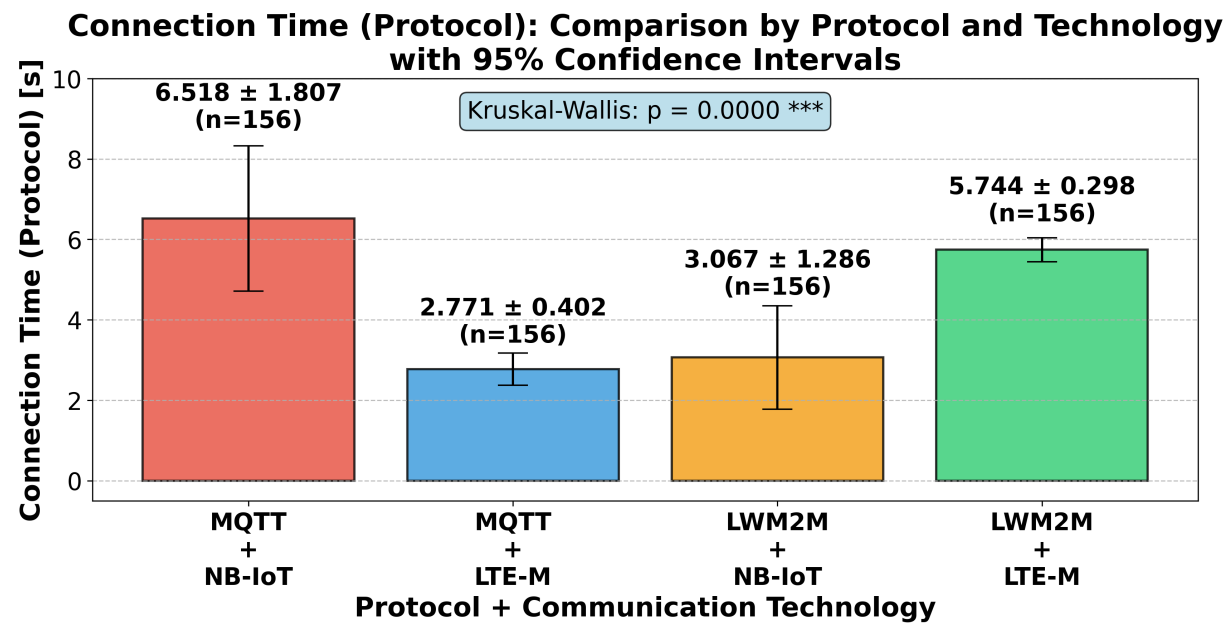
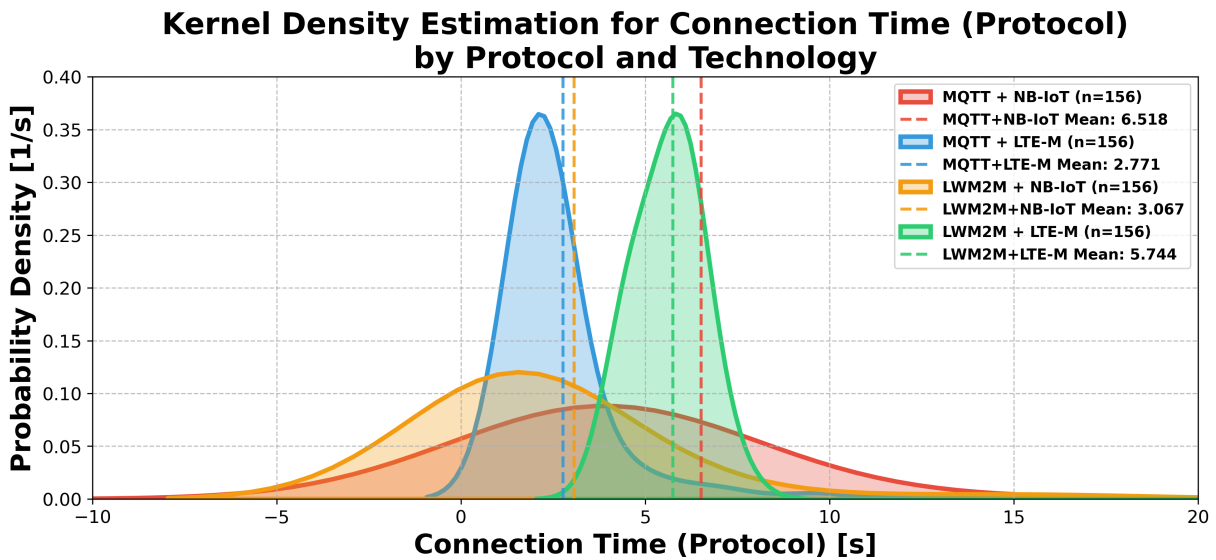


Figure 4.16: **Connection Time Distribution and Comparison**

The figure shows protocol connection time distributions (top) and confidence interval comparison (bottom) across protocol and technology combinations: MQTT+NB-IoT, MQTT+LTE-M, LWM2M+NB-IoT, and LWM2M+LTE-M.

Security Handshake Time Distribution

The security handshake time analysis, illustrated in Figure 4.17, reveals significant performance variations across protocol-technology combinations through both distribution analysis and statistical comparison. The KDE plot demonstrates that LWM2M over NB-IoT achieves the fastest security establishment with a mean handshake time of 1.021 seconds, while MQTT over NB-IoT requires the longest handshake time at 7.008 seconds. The distribution analysis shows MQTT over NB-IoT demonstrating the highest variance in handshake times, whereas LWM2M over NB-IoT shows the most consistent performance. The confidence interval comparison confirms these findings, with statistical analysis using the Kruskal-Wallis test providing highly significant differences ($p < 0.001$) in security handshake times across all combinations.

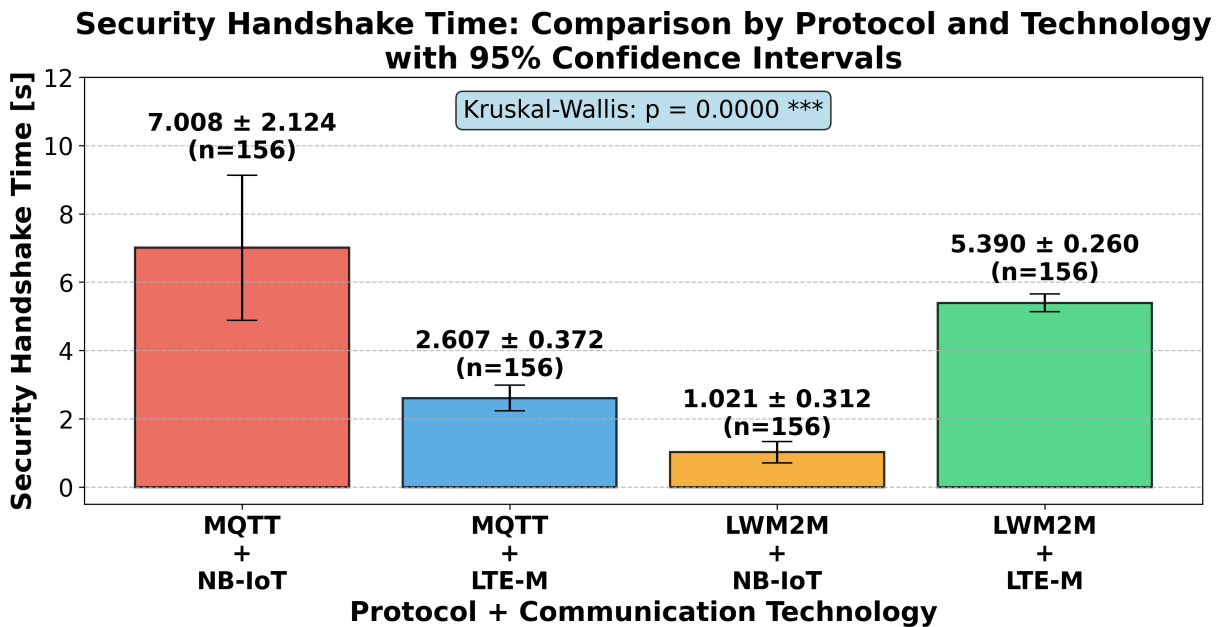
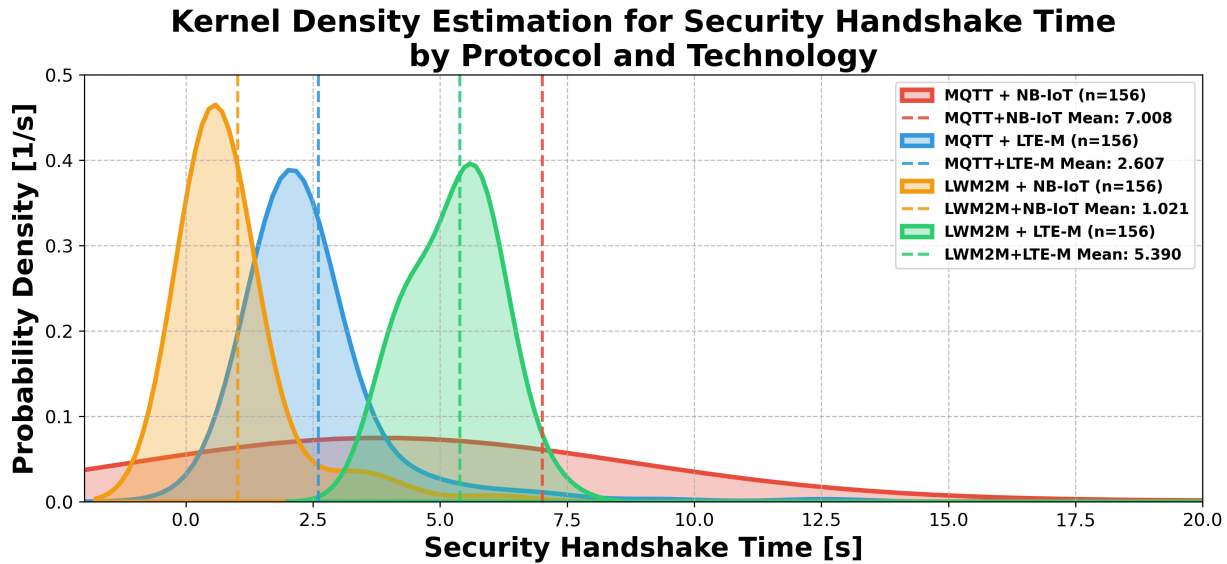


Figure 4.17: Security Handshake Time Distribution and Comparison

The figure shows the distribution (top) and confidence interval comparison (bottom) of time required for security handshake establishment across MQTT and LWM2M protocols on both NB-IoT and LTE-M technologies.

Latency Distribution

Figure 4.18 presents the latency analysis across all protocol-technology combinations, combining distribution visualization with statistical comparison. The kernel density estimation shows that MQTT over LTE-M achieves the lowest latency with a mean of 0.134 seconds, while LWM2M over NB-IoT shows substantially higher latency with a mean of 1.402 seconds. The distribution analysis reveals that LWM2M over NB-IoT demonstrates considerably higher variance compared to other combinations, while MQTT over LTE-M shows the most consistent latency performance. The confidence interval comparison confirms these observations, with the Kruskal-Wallis test providing highly significant differences ($p < 0.001$) in latency performance across combinations.

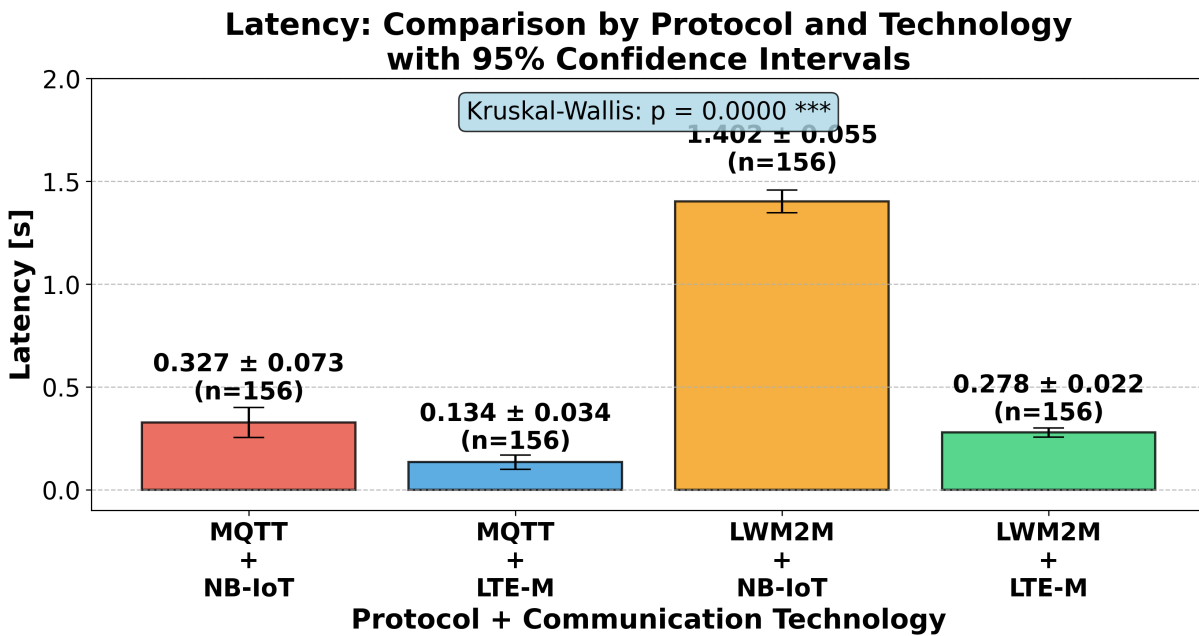
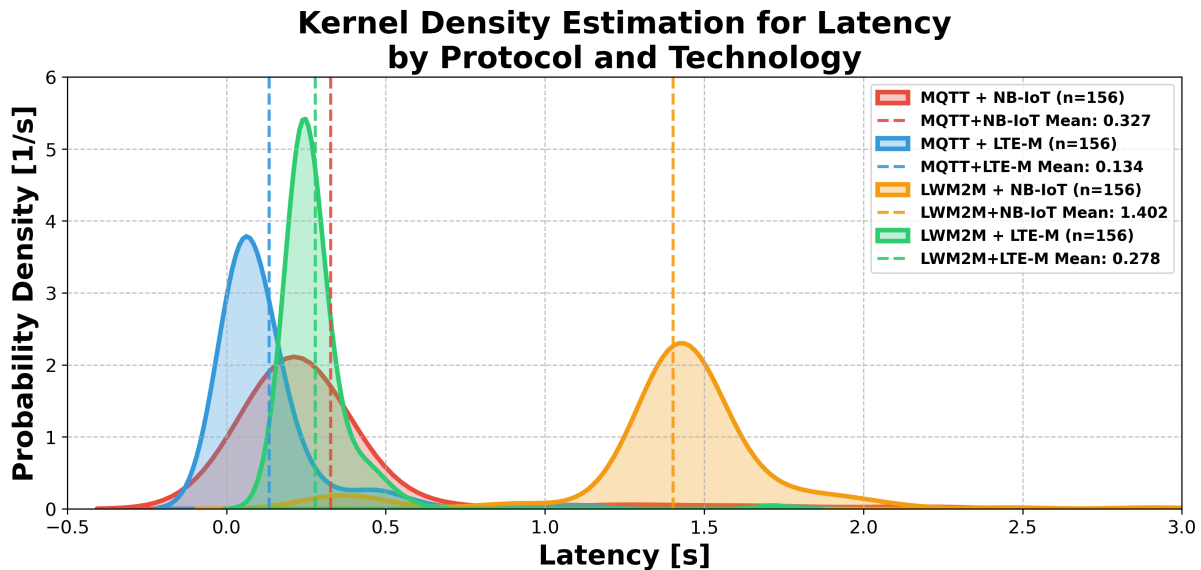


Figure 4.18: End-to-end Latency Distribution and Comparison
The figure shows latency distributions (top) and confidence interval comparison (bottom) across all four protocol-technology combinations, indicating overall system responsiveness.

Network Registration Changes Analysis

The network registration changes analysis, shown in Figure 4.19, combines distribution analysis with statistical comparison to reveal comprehensive performance characteristics. The KDE visualization shows that MQTT over NB-IoT produces the fewest network registration changes with a mean of 7.045 occurrences, while LWM2M over LTE-M generates the highest number with a mean of 15.583 changes. The distribution analysis reveals that LWM2M over LTE-M has the highest variance in registration changes, while MQTT over both LTE-M and NB-IoT demonstrate similar and relatively low variance characteristics. Statistical analysis using the Kruskal-Wallis test, displayed in the confidence interval comparison, confirms highly significant differences ($p < 0.001$) across combinations.

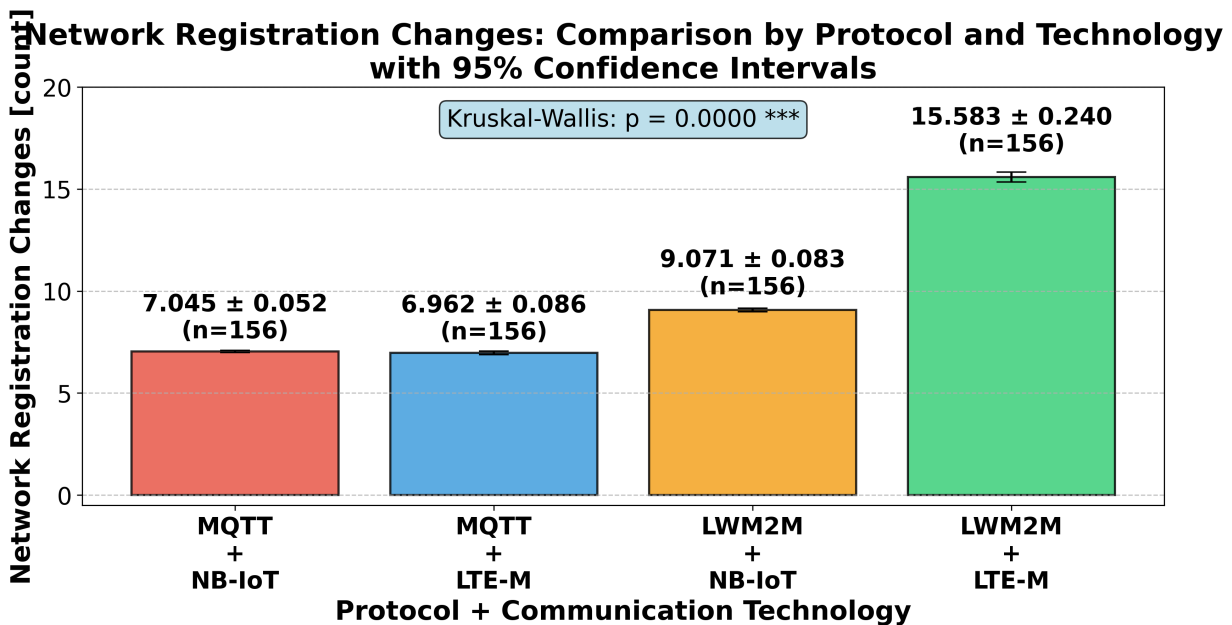
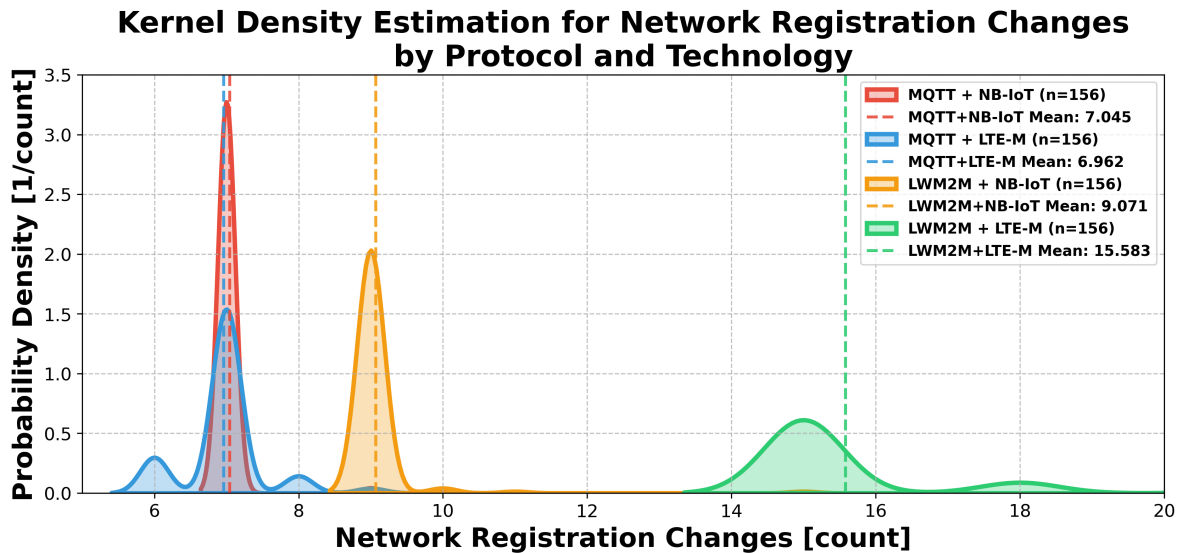


Figure 4.19: Network Registration Changes Distribution and Comparison

The figure shows the distribution (top) and confidence interval comparison (bottom) of network registration state changes during communication sessions across different protocol-technology combinations.

Retransmissions Distribution

Figure 4.20 illustrates the comprehensive retransmission analysis across protocol-technology combinations through integrated distribution and statistical visualization. The KDE analysis demonstrates that MQTT over LTE-M achieves the lowest retransmission rate with a mean of 2.109 occurrences, while LWM2M over NB-IoT requires the highest number of retransmissions with a mean of 12.833 occurrences. The distribution visualization shows that LWM2M over NB-IoT leads to the highest variance in retransmission requirements, whereas MQTT over LTE-M shows the most consistent performance with minimal variance. The confidence interval comparison confirms these findings, with the statistical analysis using the Kruskal-Wallis test showing highly significant differences ($p < 0.001$) in retransmission behavior.

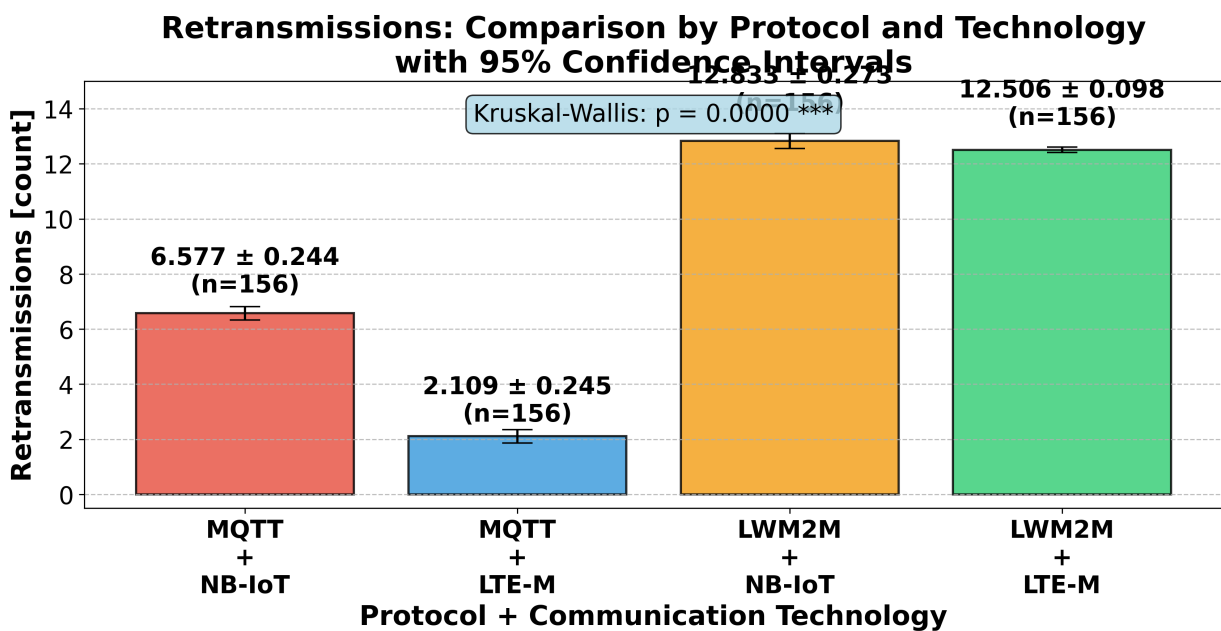
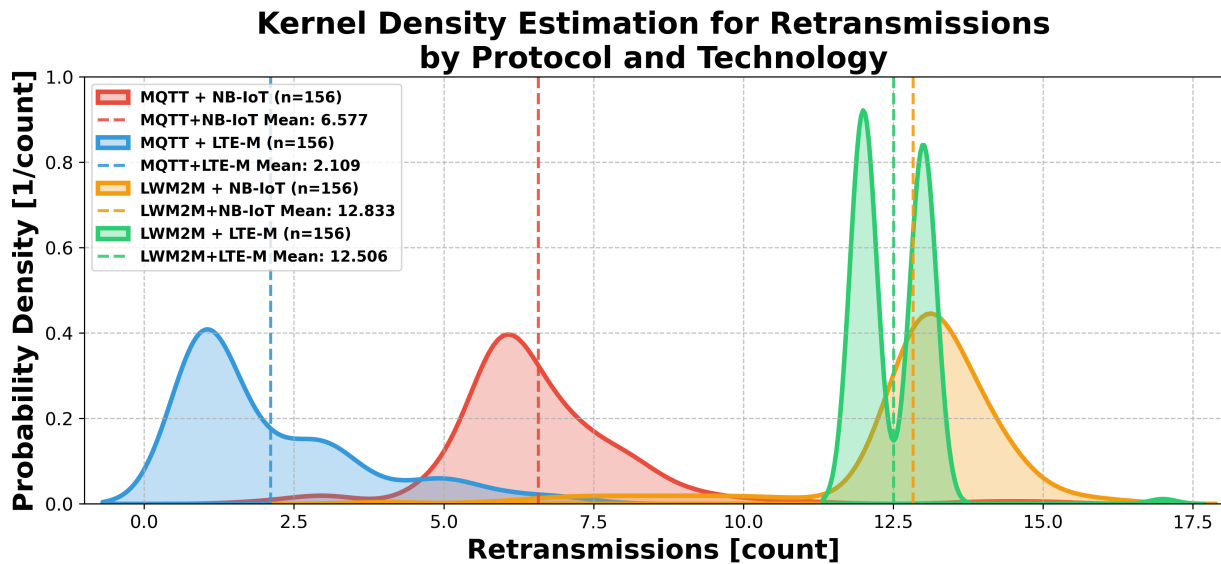


Figure 4.20: **Retransmissions Distribution and Comparison**

The figure shows the distribution (top) and confidence interval comparison (bottom) of packet retransmissions required during communication sessions, indicating link reliability and protocol efficiency across different combinations.

RRC State Changes Analysis

The RRC state changes analysis, presented in Figure 4.21, provides visualization combining distribution characteristics with statistical comparison. The kernel density estimation shows that MQTT over NB-IoT produces the fewest RRC state transitions with a mean of 2.077 occurrences, while LWM2M over LTE-M generates the most transitions with a mean of 6.154 occurrences. The distribution analysis reveals that MQTT over NB-IoT demonstrates the lowest variance in RRC state changes, indicating stable radio resource utilization, while LWM2M over LTE-M exhibits the highest variance in state transition behavior. Statistical testing using the Kruskal-Wallis test, shown in the confidence interval comparison, confirms highly significant differences ($p < 0.001$) across all combinations.

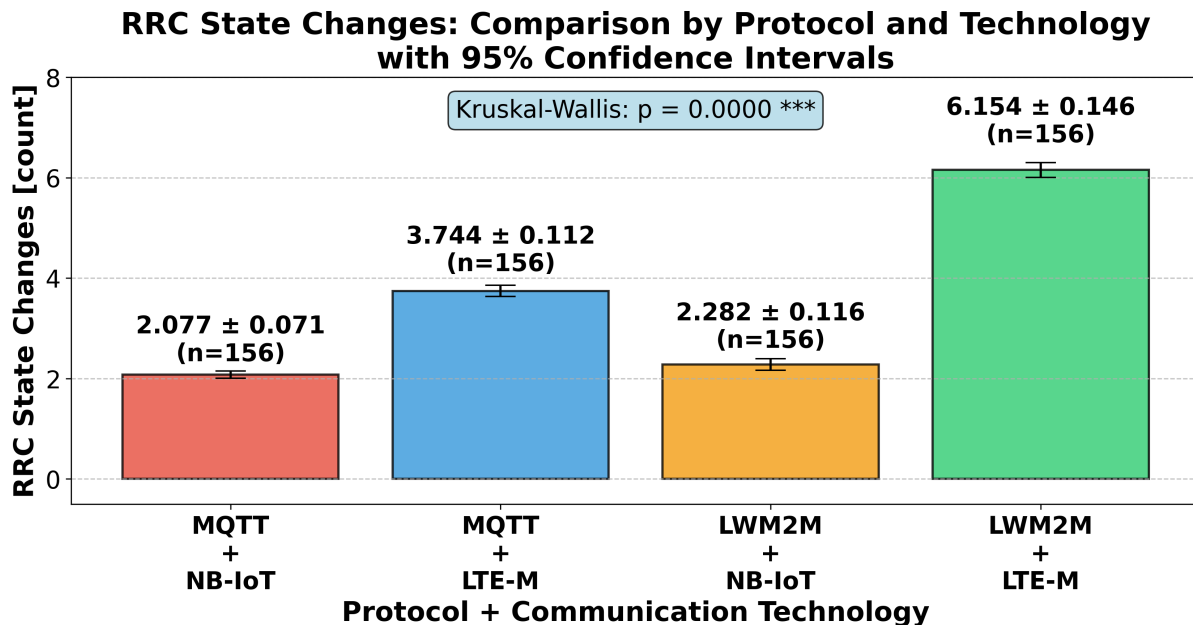
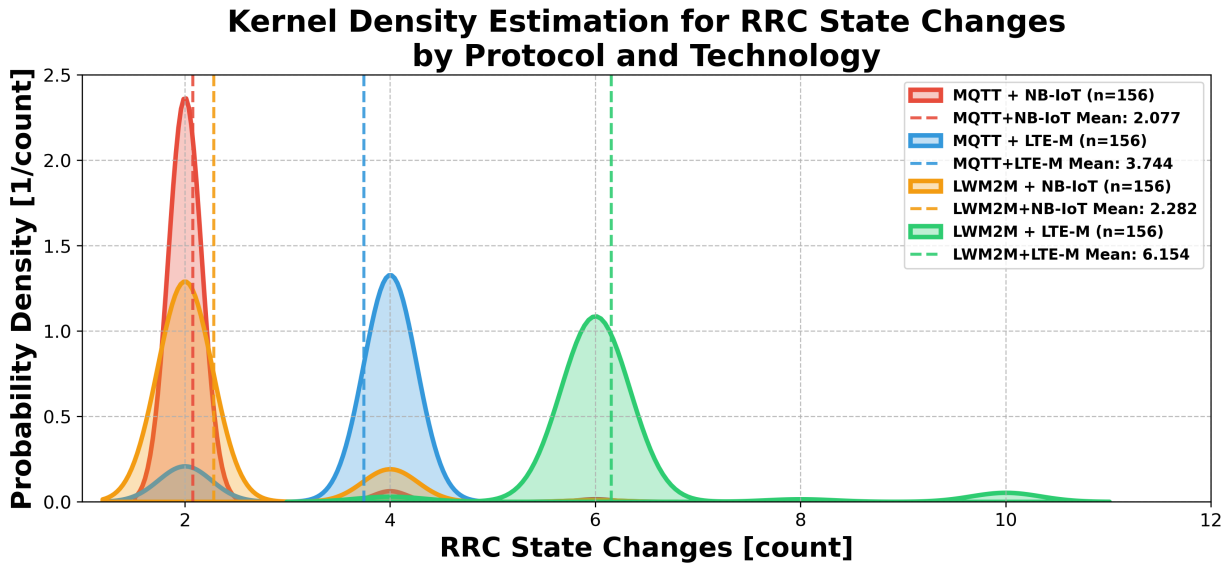


Figure 4.21: **RRC State Changes Distribution and Comparison**

The figure shows the distribution (top) and confidence interval comparison (bottom) of Radio Resource Control state transitions during communication sessions across different protocol-technology combinations.

Protocol and Technology Combination Summary

Figure 4.22 provides a full performance summary across all protocol-technology combinations, highlighting the relative strengths and weaknesses of each combination across multiple performance dimensions. The visualization allows identification of optimal combinations for specific application requirements and performance priorities.

Protocol Performance Comparison Matrix					
Metric	MQTT+NB-IoT	MQTT+LTE-M	LWM2M+NB-IoT	LWM2M+LTE-M	Key Insight
Connection time (protocol) [s]	6.518±11.428 (n=156)	2.771±2.539 (n=156)	3.067±8.132 (n=156)	5.744±1.883 (n=156)	Protocol efficiency
Latency [s]	0.327±0.460 (n=156)	0.134±0.216 (n=156)	1.402±0.347 (n=156)	0.278±0.139 (n=156)	Real-time capability
Security handshake time [s]	7.008±13.432 (n=156)	2.607±2.351 (n=156)	1.021±1.974 (n=156)	5.390±1.642 (n=156)	Security overhead
Retransmissions [count]	6.58±1.55 (n=156)	2.11±1.55 (n=156)	12.83±1.73 (n=156)	12.51±0.62 (n=156)	Protocol reliability

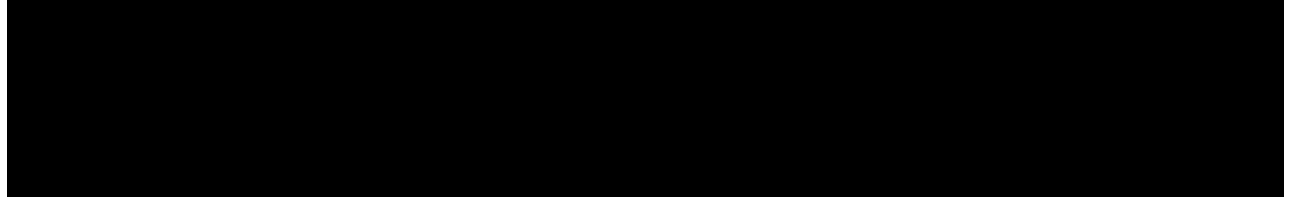


Figure 4.22: **Protocol and Technology Combination Performance Summary**

The figure summarizes the performance differences across all protocol and technology combinations. It highlights the strengths and weaknesses of each combination in terms of connection time, latency, retransmissions, and RRC state changes.

The protocol and technology combination analysis reveals distinct performance profiles for each configuration. The combined visualization approach, integrating both distribution analysis and statistical comparison, demonstrates that MQTT over LTE-M consistently achieves superior performance in latency and connection stability metrics, while LWM2M over NB-IoT shows advantages in security handshake efficiency but challenges in overall system responsiveness. These empirical findings provide essential data for informed protocol and technology selection in IoT deployment scenarios.

5. Discussion

This chapter provides an interpretation of the empirical findings presented in Chapter 4, evaluating the performance characteristics of NB-IoT and LTE-M technologies in conjunction with MQTT and LWM2M protocols for outdoor data collection deployments. The discussion intends to provide the results within the theoretical framework established in Chapter 2 and identifies both expected outcomes and surprising findings that came up during the measurements.

5.1 Interpretation of results

The measurement campaign generated a full dataset with 12 radio frequency parameters and 6 protocol-specific metrics across four distinct protocol-technology combinations. The results reveal performance profiles that align with theoretical expectations while also uncovering unexpected behaviors in real-world outdoor deployment scenarios.

5.1.1 Signal Quality and Coverage Performance

The signal quality metrics demonstrate clear differentiation between NB-IoT and LTE-M technologies. As shown in Figure 4.3, NB-IoT consistently achieves superior RSRP values with a mean approximately 6 dBm higher than LTE-M. This finding aligns with the theoretical coverage enhancement capabilities described in Section 2.1, where NB-IoT's narrowband concentration and repetition coding mechanisms provide up to 20 dB coverage improvement over standard LTE.

The frequency analysis reveals that both technologies share Band 20 (800 MHz range) while utilizing different additional frequency bands. NB-IoT operates on Band 8 (880-915 MHz uplink, 925-960 MHz downlink) while LTE-M utilizes Band 3 (1710-1785 MHz uplink, 1805-1880 MHz downlink). This frequency allocation pattern contributes to the observed signal quality differences, as the lower frequency bands generally provide better propagation characteristics for outdoor deployments. The shared use of Band 20 by both technologies demonstrates similar performance characteristics in this frequency range, while the additional bands reveal technology-specific optimization strategies.

Similarly, the RSRQ and SNR analyses presented in Figures 4.4 and 4.5 confirm NB-IoT's signal quality advantages, with mean improvements of 3.5 dB and 3 dB respectively. These results validate the theoretical framework outlined in Section 2.5, where NB-IoT's 180 kHz narrowband operation concentrates energy more effectively than LTE-M's 1.4 MHz bandwidth allocation.

However, an unexpected finding emerged in the variance characteristics of these metrics. While both technologies demonstrate similar RSRP variance, LTE-M shows notably higher RSRQ variance, suggesting more variable signal quality conditions. This contrasts with theoretical expectations that LTE-M's wider bandwidth would provide more stable signal conditions. The higher variance in LTE-M's signal quality metrics may be partially attributed to its operation across both lower frequency Band 20 and higher frequency Band 3, which experience different propagation characteristics and interference patterns in outdoor environments.

5.1.2 Power Consumption and Energy Efficiency

The transmit power analysis in Figure 4.2 reveals that LTE-M requires approximately 3 dBm higher transmit power than NB-IoT, confirming theoretical predictions about NB-IoT's energy efficiency advantages. This finding is particularly significant for outdoor deployments where sensor nodes must operate on battery power for extended periods in remote locations, as the 3 dBm difference translates to approximately double the power consumption for LTE-M transmissions.

The energy estimate distributions shown in Figure 4.8 present a discrete pattern with three distinct peaks for both technologies. This finding reflects the categorical nature of the energy estimate parameter, which is encoded as discrete integer values by the modem rather than continuous measurements. The observed distribution pattern indicates that both technologies mostly operate within three specific energy consumption classes, likely corresponding to different coverage enhancement levels or network optimization states implemented by the cellular operator.

5.1.3 Connection Establishment and Throughput Performance

The connection time analysis in Figure 4.6 reveals one of the most significant practical differences between the technologies. NB-IoT requires approximately 6.3 seconds more for network attachment compared to LTE-M, which clearly exceeds the theoretical latency specifications outlined in Section 2.1. This finding has critical implications for outdoor applications where rapid data transmission may be required during brief weather windows or in response to environmental alerts.

Furthermore, the uplink throughput analysis in Figure 4.11 confirms theoretical expectations, with LTE-M achieving approximately 215 kbps higher uplink throughput than NB-IoT. The data shows NB-IoT consistently operating within 0-100 kbps, while LTE-M demonstrates a peak around 300 kbps with a broad uplink distribution spanning 100-380 kbps, aligning closely with theoretical uplink specifications of up to 375 kbps described in Section 2.2.

5.1.4 Limitations of the Study

While this study provides empirical data on LPWAN technology and protocol performance for outdoor data collection applications, several limitations must be acknowledged to better understand the findings.

Geographic and Environmental Constraints

The measurement campaign was conducted within a specific geographic region around Cologne, Germany, which may limit the overall generalization of findings to other outdoor deployment environments. Figure 4.1 shows the spatial distribution of measurement points, which primarily covers urban and suburban environments. The results may not reflect performance characteristics in:

Rural and Remote Areas: Where outdoor experiments and environmental monitoring are commonly executed and cellular coverage characteristics, cell tower density, and interference patterns differ significantly from the measured urban/suburban environment.

Different Climatic Conditions: The measurements were conducted under specific weather and seasonal conditions that may influence radio propagation characteristics relevant to long-term outdoor deployments.

International Variations: Different countries employ varying frequency band allocations, network optimization strategies, and infrastructure deployment patterns that could significantly impact performance metrics for global outdoor monitoring deployments.

Measurement Methodology Limitations

A number of elements of the measurement approach result in limitations on the interpretation of results for applications in outdoor data collection:

Single Measurement Per Location: The study collected only one measurement per geographic location, which may not adequately capture the temporal variability in network performance that outdoor sensors would experience over extended deployment periods. Multiple measurements at each location would have provided better statistical averaging and reduced the impact of temporary network conditions or outlier performance events that could significantly affect long-term outdoor monitoring reliability.

Limited Sample Size: While statistically significant, the overall sample sizes for some parameter combinations may be insufficient to capture important performance events that could significantly impact long-term outdoor deployments. Larger sample sizes with repeated measurements would improve the statistical reliability of the findings and better represent the performance variability experienced in real outdoor monitoring scenarios.

Hardware Platform Specificity: The exclusive use of nRF9160 development kits introduces potential hardware-specific performance characteristics that may not generalize to commercial

outdoor monitoring sensor platforms or alternative IoT device implementations used in environmental research.

Protocol Implementation Variations: The study utilized specific firmware implementations of MQTT and LWM2M protocols that may not fit to the performance characteristics of optimized commercial implementations used in outdoor monitoring systems.

Traffic Pattern Limitations: The measurement scenarios used fixed payload sizes and transmission patterns that may not accurately represent the diverse data transmission characteristics of real outdoor applications. These characteristics may include variable sensor data sizes, image transmission, or burst data collection patterns.

6. Conclusion

This thesis has conducted a comprehensive performance evaluation of NB-IoT and LTE-M technologies in conjunction with MQTT and LWM2M protocols for outdoor data collection deployments. Through systematic measurement campaigns and empirical analysis across multiple geographic locations, the study provides evidence-based insights into the practical performance characteristics of these technologies under real-world outdoor conditions.

6.1 Summary of Findings

The empirical investigation reveals distinct performance profiles for each technology-protocol combination, with significant implications for outdoor deployment strategies.

6.1.1 Communication Technology Performance

The comparison between NB-IoT and LTE-M demonstrates clear performance differentiation across multiple dimensions:

NB-IoT Advantages: NB-IoT consistently outperforms LTE-M in signal quality metrics, achieving mean improvements of 6 dBm in RSRP, 3.5 dB in RSRQ, and 3 dB in SNR. The technology requires approximately 3 dBm lower transmit power, translating to significant energy efficiency advantages for battery-powered outdoor sensors. These findings validate theoretical coverage enhancement claims and confirm NB-IoT's suitability for challenging outdoor environments where long-term autonomous operation is prioritized.

LTE-M Advantages: LTE-M demonstrates superior performance in connection establishment and uplink data throughput capabilities. The technology achieves network attachment approximately 6.3 seconds faster than NB-IoT and provides 215 kbps higher average uplink throughput, with peak uplink performance reaching 300-380 kbps compared to NB-IoT's 0-100 kbps range. These characteristics position LTE-M favorably for outdoor applications requiring responsive data transmission or moderate bandwidth requirements.

Operational Trade-offs: The analysis reveals fundamental trade-offs between energy efficiency and performance responsiveness. While NB-IoT offers superior signal quality and energy characteristics, it requires additional transmission repetitions and exhibits higher connection latency. In contrast, LTE-M provides faster, more consistent connectivity at the cost of increased power consumption.

6.1.2 Protocol Performance Across Technologies

The four-way comparison presented in Figure 4.22 reveals that protocol performance is highly dependent on the underlying cellular technology, creating distinct optimization domains for different outdoor deployment scenarios.

MQTT Performance Profile:

MQTT demonstrates its most favorable performance when paired with LTE-M, achieving the lowest latency and connection establishment times across all combinations. However, MQTT performance degrades significantly on NB-IoT, requiring the longest connection and security handshake times. This degradation suggests that MQTT's TCP overhead becomes prohibitive on bandwidth-constrained networks, contradicting theoretical assumptions about protocol scalability.

LWM2M Performance Profile:

LWM2M shows unexpectedly poor performance on NB-IoT despite theoretical advantages of UDP-based transport. The combination produces the highest end-to-end latency and retransmission rates, indicating that CoAP's reliability mechanisms may interact poorly with NB-IoT's repetition coding mechanisms. This finding challenges theoretical assumptions about UDP efficiency on constrained networks and suggests that CoAP's confirmable message semantics may become counterproductive under certain conditions.

Session Duration and Protocol Overhead Impact:

A significant element leading to the surprising performance of the UDP protocol is the short session duration. The experimental design used very small data payloads and short communication sessions, which reduced the likelihood of connection losses during transmission. Given that TCP is sensitive to connection interruptions, where each loss would trigger the overhead of a new handshake, shorter sessions can help minimize the occurrence of this weakness. In such scenarios, the probability of connection loss is reduced, meaning that TCP's handshake overhead is less frequently experienced. Consequently, the potential efficiency advantage of UDP's connectionless design becomes less significant in the payload sizes and transmission patterns evaluated in this study.

6.1.3 Technology and Protocol Recommendations

Based on the empirical findings, this study provides evidence-based recommendations for technology selection and deployment strategies in outdoor data collection scenarios.

For Long-term Environmental Monitoring: The deployment of NB-IoT technology for stationary outdoor sensors necessitates an optimal battery life and reliable connectivity, especially in challenging environments. This technology is well-suited for long-term environmental studies, remote agricultural monitoring, and applications with minimal latency requirements.

For Responsive Environmental Applications: Utilize LTE-M for outdoor applications requiring regular connectivity, moderate data rates, or time-sensitive responses. Recommended

for real-time environmental alert systems, automated response systems, and research installations requiring frequent data transmission.

For Hybrid Deployment Strategies: Organizations conducting diverse outdoor monitoring activities should consider multi-technology approaches, pushing each technology's strengths for appropriate use cases within the same deployment area.

Protocol Selection Recommendations:

MQTT + LTE-M: Recommended as the primary combination for outdoor applications requiring low-latency sensor data transmission, integration with established IoT ecosystems, and moderate data rates. The combination provides the most predictable and efficient performance profile for responsive environmental monitoring systems.

LWM2M + LTE-M: Suitable for outdoor monitoring systems requiring remote device management capabilities, firmware updates, and complex configuration management.

MQTT + NB-IoT: Use only for applications with minimal latency requirements and infrequent communication patterns, such as daily environmental logging.

LWM2M + NB-IoT: Generally not recommended due to poor latency performance and high retransmission rates, except for specialized device management scenarios where security handshake efficiency is prioritized.

6.1.4 Research Contributions

This thesis makes several significant contributions to the understanding of LPWAN technology performance for outdoor data collection applications:

Empirical Evaluation: The study provides empirical evaluation that simultaneously examines both communication technology performance (NB-IoT vs. LTE-M) and protocol behavior (MQTT vs. LWM2M) under identical outdoor conditions, addressing a critical gap in existing literature.

Protocol-Technology Interaction Analysis: The identification and quantification of protocol-technology interaction dependencies provides new insights that challenge conventional assumptions about protocol efficiency on constrained networks, particularly the unexpected poor performance of UDP-based protocols on bandwidth-constrained networks.

Real-World Performance Validation: The empirical validation of theoretical specifications has revealed significant differences between standardized performance specifications and practical deployment reality, providing valuable data for future standardization efforts and deployment planning.

Statistical Performance Characterization: The statistical analysis using Mann-Whitney U and Kruskal-Wallis tests provides robust validation of the observed performance differences, ensuring confidence in the practical significance of the findings.

Methodological Framework: The development of a reproducible measurement framework and automated data collection system provides a foundation for future research in outdoor

LPWAN performance evaluation.

7. Outlook

This chapter presents an overview of future advancements and potential enhancements in the area of outdoor data collection using LPWAN technologies.

While this study provides a detailed performance characterization of NB-IoT and LTE-M in combination with MQTT and LWM2M for outdoor data collection, several extensions could enhance the applicability and generality of the findings. Future research should include repeated measurements at each location to capture temporal variability and enhance statistical reliability. The geographic scope should be expanded to include rural and remote areas, and multi-operator evaluations should be performed to provide broader coverage of real-world deployment conditions. The use of diverse hardware platforms and the implementation of optimized commercial protocols could potentially reveal hardware- and software-specific effects that were not captured in this study. Furthermore, integrating variable payload sizes and more authentic traffic patterns would facilitate performance evaluation under a broader spectrum of operational scenarios relevant to outdoor monitoring applications.

A notable observation in this study was that the short session duration and very small payload sizes reduced the likelihood of connection losses during transmission. Given the sensitivity of TCP to connection interruptions, where each loss triggers the overhead of a new handshake, shorter sessions have been shown to minimize the occurrence of this weakness. Therefore, TCP's handshake overhead was barely experienced, and the potential efficiency advantage of UDP's connectionless design became less significant under the tested conditions. To further investigate this effect, future experiments should include longer connection sessions and varied payload sizes to evaluate whether differences in UDP and TCP performance become more apparent when connection losses are more likely to occur. Such investigations would help clarify protocol behavior in deployment scenarios involving continued data flows or more challenging network conditions.

Tools Used

In the course of creating this work, the following tools and resources were used to assist:

- ChatGPT (OpenAI)
- Claude Sonnet (Anthropic)
- DeepL Translator
- MacTex
- VS Code (Visual Studio Code)
- GitHub Copilot

8. Acknowledgements

I would like to thank everyone who supported and encouraged me during the preparation of this master's thesis.

First, I am grateful to Professor Dr. Uwe Dettmar for supervising my work and for his valuable guidance in developing ideas over the past years. I would also like to thank my colleagues and fellow students at the Institute of Digital Communication for their constructive discussions and practical advice.

Special thanks go to Dipl.-Ing. Martin Seckler for his patient and reliable help with numerous measurements and technical challenges, and to Professor Dr. Harald Elders-Boll for serving as co-examiner.

Finally, I am deeply thankful to my parents, my brother, and my friends for their support throughout my studies.

Erklärung

Ich versichere, die von mir vorgelegte Arbeit selbstständig verfasst zu haben. Alle Stellen, die wörtlich oder sinngemäß aus veröffentlichten oder nicht veröffentlichten Arbeiten anderer oder der Verfasserin/des Verfassers selbst entnommen sind, habe ich als entnommen kenntlich gemacht. Sämtliche Quellen und Hilfsmittel, die ich für die Arbeit benutzt habe, sind angegeben. Die Arbeit hat mit gleichem Inhalt bzw. in wesentlichen Teilen noch keiner anderen Prüfungsbehörde vorgelegen.

Ort, Datum

Unterschrift

List of Figures

2.1	MQTT Connection Establishment The picture shows the typical phases of the client-broker connection in MQTT. [1]	15
2.2	MQTT Messaging The picture shows the behavior when transmitting messages with different QoS parameters. [1]	16
3.1	nRF9160 Development Kit Nordic Semiconductor nRF9160 Development Kit showing the main circuit board with integrated cellular and GPS antennas, USB connector, and development interface pins.	23
4.1	Data Collection Locations The figure shows the distribution of the 156 measurement locations. Each marker represents a single conducted measurement.	32
4.2	TX Power Distribution The figure shows the transmit power distribution for NB-IoT and LTE-M technologies. Lower TX power indicates better energy efficiency and coverage conditions.	40
4.3	RSRP Distribution The figure shows RSRP values measured across different locations. Higher RSRP values indicate better signal coverage and link quality.	41
4.4	RSRQ Distribution The figure shows RSRQ measurements comparing NB-IoT and LTE-M signal quality. RSRQ reflects the quality of the received reference signal.	42
4.5	SNR Distribution The figure shows SNR measurements for both technologies. Higher SNR values indicate better signal quality and more reliable communication.	43
4.6	Link Connection Time Distribution The figure shows the time required to establish cellular network connectivity. Lower connection times indicate faster network attachment and improved user experience.	44
4.7	Downlink Pathloss Distribution The figure shows signal attenuation in the downlink path for both NB-IoT and LTE-M. Lower pathloss values indicate better propagation conditions.	45
4.8	Energy Estimate Distribution The figure shows relative energy consumption estimates for data transmission. Lower values indicate more energy-efficient communication.	46
4.9	RX Repetitions Distribution The figure shows the number of receive repetitions required for reliable communication. Higher repetitions indicate poorer link conditions.	47

4.10	TX Repetitions Distribution The figure shows the number of transmission repetitions required for reliable uplink communication. Higher repetitions indicate coverage enhancement needs.	48
4.11	Link Throughput Distribution The figure shows achieved data throughput for NB-IoT and LTE-M connections. Higher throughput values indicate better data transmission performance.	49
4.12	Uplink Frequency Distribution The figure shows the uplink frequencies used for NB-IoT and LTE-M connections. Frequencies are derived from EARFCN values and reflect the radio access technology used.	50
4.13	Downlink Frequency Distribution The figure shows the downlink frequencies used for NB-IoT and LTE-M connections. Frequencies are derived from EARFCN values and reflect the radio access technology used.	51
4.14	Technology Comparison Radar Chart The figure provides a multi-dimensional comparison of NB-IoT and LTE-M across various performance metrics. The left radar chart shows metrics where higher values indicate better performance, while the right radar chart shows metrics where lower values indicate better performance.	52
4.15	Communication Technology Comparison Summary The figure summarizes the performance differences between NB-IoT and LTE-M across key metrics. It highlights the strengths and weaknesses of each technology in terms of signal quality, connection time, and energy efficiency.	53
4.16	Connection Time Distribution and Comparison The figure shows protocol connection time distributions (top) and confidence interval comparison (bottom) across protocol and technology combinations: MQTT+NB-IoT, MQTT+LTE-M, LWM2M+NB-IoT, and LWM2M+LTE-M.	55
4.17	Security Handshake Time Distribution and Comparison The figure shows the distribution (top) and confidence interval comparison (bottom) of time required for security handshake establishment across MQTT and LWM2M protocols on both NB-IoT and LTE-M technologies.	57
4.18	End-to-end Latency Distribution and Comparison The figure shows latency distributions (top) and confidence interval comparison (bottom) across all four protocol-technology combinations, indicating overall system responsiveness.	59
4.19	Network Registration Changes Distribution and Comparison The figure shows the distribution (top) and confidence interval comparison (bottom) of network registration state changes during communication sessions across different protocol-technology combinations.	61

4.20 Retransmissions Distribution and Comparison The figure shows the distribution (top) and confidence interval comparison (bottom) of packet retransmissions required during communication sessions, indicating link reliability and protocol efficiency across different combinations.	63
4.21 RRC State Changes Distribution and Comparison The figure shows the distribution (top) and confidence interval comparison (bottom) of Radio Resource Control state transitions during communication sessions across different protocol-technology combinations.	65
4.22 Protocol and Technology Combination Performance Summary The figure summarizes the performance differences across all protocol and technology combinations. It highlights the strengths and weaknesses of each combination in terms of connection time, latency, retransmissions, and RRC state changes.	66

List of Tables

2.1 Comparison of Key Features between LTE-M and NB-IoT	19
2.2 Comparison of Key Features between LwM2M and MQTT	21

Acronyms

3GPP 3rd Generation Partnership Project. 6, 8, 9, 11

AES Advanced Encryption Standard. 8, 11

AGNSS Assisted GNSS. 24

AKA Authentication and Key Agreement. 8, 11

API Application Programming Interface. 35

APN Access Point Name. 27

BLE Bluetooth Low Energy. 22

BPSK Binary Phase Shift Keying. 7

CE Coverage Enhancement. 27

CoAP Constrained Application Protocol. 17–19, 31, 33, 72

DL Downlink. 27

DTLS Datagram Transport Layer Security. 18, 19, 24, 33

EARFCN E-UTRA Absolute Radio Frequency Channel Number. 27

eDRX Extended Discontinuous Reception. 8, 12, 27

FEC Forward Error Correction. 7, 10

FOTA Firmware Over-The-Air. 11

GNSS Global Navigation Satellite System. 22, 24–26, 28

GPS Global Positioning System. 22, 25, 28, 30

GSM Global System for Mobile Communications. 6

HARQ Hybrid Automatic Repeat reQuest. 9, 10

- HTTP** Hypertext Transfer Protocol. 2
- IoT** Internet of Things. 2, 5–9, 11, 13, 17, 19, 22, 24, 66, 70, 73
- IP** Internet Protocol. 29
- KDE** Kernel Density Estimation. 37, 38, 40, 54
- LPWAN** Low Power Wide Area Network. 1, 2, 9, 69, 73–75
- LTE** Long Term Evolution. 1–4, 6–12, 67
- LTE-M** Long Term Evolution for Machines. 2, 5, 9–12, 22, 26, 27, 36–55, 57, 58, 60, 62, 64, 66–68, 71–73, 75, 77, 78
- LWM2M** Lightweight Machine to Machine. 1, 2, 4, 5, 17–19, 22, 24–28, 31, 33, 34, 37, 39, 54–58, 60, 62, 64, 66, 67, 70–73, 75, 78
- M2M** Machine to Machine. 13
- MCC** Mobile Country Code. 27
- mMTC** Massive Machine-Type Communication. 6
- MNC** Mobile Network Code. 27
- MQTT** Message Queuing Telemetry Transport. 1, 2, 4, 5, 13–15, 17, 18, 22, 24–26, 28, 33–35, 37, 39, 54–58, 60, 62, 64, 66, 67, 70–73, 75, 77, 78
- NAS** Non-Access Stratum. 34
- NB-IoT** Narrowband Internet of Things. 1–12, 22, 26, 27, 29, 36–58, 60, 62, 64, 66–68, 71–73, 75, 77, 78
- NFC** Near Field Communication. 22
- OFDM** Orthogonal Frequency Division Multiplexing. 10
- OFDMA** Orthogonal Frequency Division Multiple Access. 7
- PAPR** Peak-to-Average Power Ratio. 7
- PCAP** Packet Capture. 31, 33–35
- PRB** Physical Resource Block. 6, 10

PSK Pre-Shared Key. 2, 24

PSM Power Saving Mode. 8, 12

QAM Quadrature Amplitude Modulation. 10, 12

QoS Quality of Service. 14, 16, 18, 26, 77

QPSK Quadrature Phase Shift Keying. 7, 10

RRC Radio Resource Control. 2, 3, 33, 34

RSRP Reference Signal Received Power. 27, 40, 41, 52, 67, 71, 77

RSRQ Reference Signal Received Quality. 27, 41, 42, 52, 71, 77

RTOS Real-Time Operating System. 24

SC-FDMA Single Carrier Frequency Division Multiple Access. 7, 10

SDK Software Development Kit. 24

SNOW SNOW 3G. 8, 11

SNR Signal-to-Noise Ratio. 7, 27, 42, 43, 52, 71, 77

SoC System on a Chip. 22

SUPL Secure User Plane Location. 24, 26

TAC Tracking Area Code. 27

TAU Tracking Area Update. 27

TCP Transmission Control Protocol. 13, 14, 17, 31, 33, 72, 75

TLS Transport Layer Security. 14, 17, 25, 33

TTFF Time to First Fix. 24, 26

UART Universal Asynchronous Receiver-Transmitter. 24, 25, 27

UDP User Datagram Protocol. 17–19, 28, 29, 31, 33, 72, 73, 75

VCOM Virtual COM Port. 25, 28

VoLTE Voice over LTE. 9, 11

WiFi Wireless Fidelity. 1

Bibliography

- [1] Ravi Kishore Kodali and SreeRamya Soratkal. "MQTT based Home Automation System Using ESP8266". In: *2016 IEEE Region 10 Humanitarian Technology Conference (R10-HTC)*. Accessed Aug 13, 2025. National Institute Of Technology, Warangal. Warangal, India, 2016. URL: https://www.researchgate.net/publication/316448543_MQTT_based_home_automation_system_using_ESP8266.
- [2] Mads Lauridsen et al. "Coverage and Capacity Analysis of LTE-M and NB-IoT in a Rural Area". In: *2016 IEEE 84th Vehicular Technology Conference (VTC-Fall)*. Date of Conference: 18-21 September 2016; Date Added to IEEE Xplore: 20 March 2017. Montreal, QC, Canada: IEEE, Sept. 2016. ISBN: 978-1-5090-1701-0. DOI: 10.1109/VTCFa.2016.7880946. URL: <https://ieeexplore.ieee.org/document/7880946>.
- [3] Rapeepat Ratasuk et al. "NB-IoT system for M2M communication". In: *2016 IEEE Wireless Communications and Networking Conference Workshops (WCNCW)*. Date of Conference: 03-06 April 2016; Date Added to IEEE Xplore: 29 August 2016; PoD ISBN: 978-1-4673-8667-8. Doha, Qatar: IEEE, Apr. 2016. ISBN: 978-1-4673-8666-1. DOI: 10.1109/WCNCW.2016.7552737. URL: <https://ieeexplore.ieee.org/document/7552737>.
- [4] Nitin Naik. "Choice of effective messaging protocols for IoT systems: MQTT, CoAP, AMQP and HTTP". In: *2017 IEEE International Systems Engineering Symposium (ISSE)*. Date of Conference: 11-13 October 2017; Date Added to IEEE Xplore: 30 October 2017. Vienna, Austria: IEEE, Oct. 2017. DOI: 10.1109/SysEng.2017.8088251. URL: <https://ieeexplore.ieee.org/document/8088251>.
- [5] Rapeepat Ratasuk et al. "LTE-M Evolution Towards 5G Massive MTC". In: *2017 IEEE Globecom Workshops (GC Wkshps)*. Date of Conference: 04-08 December 2017; Date Added to IEEE Xplore: 25 January 2018. Singapore: IEEE, Dec. 2017. DOI: 10.1109/GLOCOMW.2017.8269112. URL: <https://ieeexplore.ieee.org/document/8269112>.
- [6] Pascal Jörke, Robert Falkenberg, and Christian Wietfeld. "Power Consumption Analysis of NB-IoT and eMTC in Challenging Smart City Environments". In: *2018 IEEE Globecom Workshops (GC Wkshps)*. Date of Conference: 09-13 December 2018; Date Added to IEEE Xplore: 21 February 2019. Abu Dhabi, United Arab Emirates: IEEE, Dec. 2018. DOI: 10.1109/GLOCOMW.2018.8644481. URL: <https://ieeexplore.ieee.org/document/8644481>.
- [7] OMA SpecWorks. *Lightweight Machine to Machine Technical Specification: Core*. Tech. rep. Open Mobile Alliance, 2019. URL: https://www.openmobilealliance.org/release/LightweightM2M/V1_1_1-20190617-A/OMA-TS-LightweightM2M_Core-V1_1_1-20190617-A.pdf.

- [8] Matthieu Kanj, Vincent Savaux, and Mathieu Le Guen. “A Tutorial on NB-IoT Physical Layer Design”. In: *IEEE Communications Surveys Tutorials* 22.4 (Sept. 2020). Date of Publication: 11 September 2020, pp. 2408–2446. DOI: 10.1109/COMST.2020.3022751. URL: <https://ieeexplore.ieee.org/document/9194757>.
- [9] Alessandro Parmigiani and Uwe Dettmar. “Comparison and Evaluation of LwM2M and MQTT in Low-Power Wide-Area Networks”. In: *2021 IEEE International Conference on Internet of Things and Intelligence Systems (IoTaIS)*. Date of Conference: 23-24 November 2021; Date Added to IEEE Xplore: 07 December 2021; USB ISBN: 978-1-6654-2034-1; PoD ISBN: 978-1-6654-2036-5. Bandung, Indonesia: IEEE, Nov. 2021. ISBN: 978-1-6654-2035-8. DOI: 10.1109/IoTaIS53735.2021.9628463. URL: <https://ieeexplore.ieee.org/document/9628463>.
- [10] Rebecca Bevans. *Understanding Confidence Intervals / Easy Examples & Formulas*. 2023. URL: <https://www.scribbr.co.uk/stats/confidence-interval-meaning/#:~:text=using%20confidence%20intervals-,What%20exactly%20is%20a%20confidence%20interval?,specified%20by%20the%20confidence%20interval.&text=So%20if%20you%20use%20an,=%200.95%2C%20or%2095%25..>
- [11] Jaroslaw Drapala. “Kernel Density Estimation explained step by step”. In: (2023). URL: <https://towardsdatascience.com/kernel-density-estimation-explained-step-by-step-7cc5b5bc4517/>.
- [12] MSc Olivia Guy-Evans. *P-Value And Statistical Significance: What It Is & Why It Matters*. 2023. URL: <https://www.simplypsychology.org/p-value.html>.
- [13] Viktoria Vomhoff et al. “NB-IoT vs. LTE-M: Measurement Study of the Energy Consumption of LPWAN Technologies”. In: *2023 IEEE International Conference on Communications Workshops (ICC Workshops)*. Date of Conference: 28 May 2023 - 01 June 2023; Date Added to IEEE Xplore: 23 October 2023. Rome, Italy: IEEE, May 2023. ISBN: 979-8-3503-3307-7. DOI: 10.1109/ICCWorkshops57953.2023.10283595. URL: <https://ieeexplore.ieee.org/document/10283595>.
- [14] Viktoria Vomhoff et al. “NB-IoT vs. LTE-M: Measurement Study of the Energy Consumption of LPWAN Technologies”. In: *2023 IEEE International Conference on Communications Workshops (ICC Workshops)*. Date of Conference: 28 May 2023 - 01 June 2023; Date Added to IEEE Xplore: 23 October 2023. Rome, Italy: IEEE, May 2023. ISBN: 979-8-3503-3307-7. DOI: 10.1109/ICCWorkshops57953.2023.10283595. URL: <https://ieeexplore.ieee.org/document/10283595>.
- [15] Wikipedia. *Kruskal-Wallis-Test*. 2023. URL: <https://de.wikipedia.org/wiki/Kruskal-Wallis-Test>.
- [16] Elliot McClenaghan. *Mann-Whitney U Test: Assumptions and Example*. 2025. URL: <https://www.technologynetworks.com/informatics/articles/mann-whitney-u-test-assumptions-and-example-363425>.

- [17] Nordic Semiconductor. *Network registration status notification +CEREG*. 2025. URL: https://docs.nordicsemi.com/bundle/ref_at_commands/page/REF/at_commands/nw_service/cereg.html.
- [18] Nordic Semiconductor. *Signaling connection status notification +CSCON*. 2025. URL: https://docs.nordicsemi.com/bundle/ref_at_commands/page/REF/at_commands/packet_domain/cscon.html.
- [19] Wikipedia. *LTE-M*. URL: <https://en.wikipedia.org/wiki/LTE-M>.
- [20] Wikipedia. *MQTT*. URL: <https://de.wikipedia.org/wiki/MQTT>.
- [21] Wikipedia. *Narrowband IoT*. URL: https://en.wikipedia.org/wiki/Narrowband_IoT.
- [22] Wikipedia. *OMA LwM2M*. URL: https://en.wikipedia.org/wiki/OMA_LWM2M.